Table 1. Anti-HCV activities of oral antifungal agents in Huh7/Rep-Feo cells [a]

	EC_{50} [b] (μM)	CC_{50} [c] (μM)	SI [d]
Griseofulvin	6.13 ± 0.17	217.93 ± 3.49	35.5
Fluconazole	135.6 ± 1.25	159.06 ± 1.07	1.2
Itraconazole	1.24 ± 0.21	3.35 ± 0.17	2.7

a. All data represent means ±standard deviation for three separate experiments.
b. Fifty percent effective concentration based on the inhibition of HCV replication.
c. Fifty percent cytotoxicity concentration based on the reduction of cell viability.
d. Selectivity Index (CC_{50}/ EC_{50}).

Early Dynamics of Hepatitis B Virus in Chimeric Mice Carrying Human Hepatocytes Monoinfected or Coinfected with Genotype G

Masaya Sugiyama,[1] Yasuhito Tanaka,[1] Tomoyuki Sakamoto,[1] Isao Maruyama,[2] Takashi Shimada,[2] Satoru Takahashi,[3] Tomoyuki Shirai,[3] Hideaki Kato,[4] Masataka Nagao,[4] Yuzo Miyakawa,[5] and Masashi Mizokami[1]

Of the 8 genotypes of HBV (genotypes A-H), genotype G is unique in that it has an insertion in the core gene and two stop codons in the precore region preventing the synthesis of hepatitis B e antigen. Most individuals with genotype G are coinfected with other genotypes, typically genotype A. Mice with severe combined immunodeficiency disease carrying human hepatocytes were infected with HBV particles propagated in Huh7 cells in culture. Mice monoinfected with genotype G did not raise detectable HBV DNA in serum, although products of the core gene emerged 4 to 8 weeks after inoculation. When they were superinfected with genotype A at week 10, however, HBV DNA of genotype A developed, which was replaced almost completely by that of genotype G within 10 weeks. Such a rapid takeover was also observed in mice initially infected with genotype A or C and superinfected with genotype G. Similar viral dynamics occurred in mice simultaneously coinfected with genotypes G and A. Takeover was markedly enhanced in mice inoculated with a serum passage containing genotype G with a trace of genotype A. Coinfection of mice with genotypes G and A induced abundant cellular steatosis along with increased fibrosis in the liver, which was not detected in mice monoinfected with genotype A or G. ***Conclusion:*** **Genotype G can monoinfect chimeric mice at very low levels, and its replication increases maredly when coinfected with other genotypes. Coinfection with genotype G could enhance fibrosis under immunocompromised states.** (HEPATOLOGY 2007;45:929-937.)

HBV infects an estimated 350 million people worldwide and causes 1 million deaths annually.[1] Eight genotypes of HBV have been classified by the sequence divergence in the entire genome exceeding 8% and have been assigned the names A through H in order of discovery.[2-6] HBV genotypes have distinct geographic distributions and can influence the severity of liver disease and response to antiviral therapies.[7-10] HBV genotypes are further divided into subgenotypes, such as A1/Aa and A2/Ae, B1/Bj and B2/Ba, and C1/Ce and C2/Cs.[11-13] These genotypes may influence clinical outcomes of HBV infection.[14,15]

HBV genotype G (HBV/G) was first described in 2000 among inhabitants of France and the state of Georgia.[5] It has an insertion of 36 base pairs in the core gene and two stop codons in the precore region.[5,16] Despite the inability in encoding hepatitis B e antigen (HBeAg), carriers of HBV/G possess it in serum.[5] They are usually coinfected with HBV of other genotypes, most frequently HBV/A, which is responsible for serum HBeAg.[17] Coinfection with HBV/C, F, and H has also been reported.[18-20] In spite of heavy dependence on other genotypes for replication, HBV/G outgrows them and eventually takes over the great majority of HBV DNA in the circulation.[16,17]

Recently, HBV/G DNA in low levels was reported in a German donor of plasmapheresis who had transmitted it to 2 recipients in look-back studies.[21] Hence, HBV/G would be able to infect recipients by itself. Furthermore,

Abbreviations: ChiM, chimeric mice; HBcrAg, HBV core-related antigen; HBeAg, hepatitis B e antigen; HBsAg, hepatitis B surface antigen; RFLP, restriction fragment length polymorphism; SCID, severe combined immunodeficiency disease.

From the [1]Department of Clinical Molecular Informative Medicine, Nagoya City University Graduate School of Medical Sciences, Nagoya, Japan; [2]PhoenixBio Co., Ltd, Higashi-Hiroshima, Japan; the Departments of [3]Experimental Pathology and Tumor Biology and [4]Forensic Medical Science, Nagoya City University Graduate School of Medical Sciences, Nagoya, Japan; and the [5]Miyakawa Memorial Research Foundation, Tokyo, Japan.

Received August 12, 2006; accepted December 1, 2006

Supported in part by a grant-in-aid from the Ministry of Health, Labor, and Welfare of Japan (H16-kanen-3), Scientific Research from the Ministry of Education (18590741), and Toyoaki Foundation.

Masaya Sugiyama and Yasuhito Tanaka contributed equally to this study.

Address reprint requests to: Masashi Mizokami, M.D., Ph.D., Department of Clinical Molecular Informative Medicine, Nagoya, City University Graduate School of Medical Sciences, Kawasumi, Mizuho, Nagoya 467-8601, Japan. E-mail: mizokami@med.nagoya-cu.ac.jp; fax: (81) 52-842-0021.

Published online in Wiley InterScience (www.interscience.wiley.com).

DOI 10.1002/hep.21584

Potential conflict of interest: Nothing to report.

Supplementary material for this article can be found on the HEPATOLOGY website (http://interscience.wiley.com/jpages/0270-9139/suppmat/index.html).

HBV/G has been detected in 25 of the 104 (24%) French patients coinfected with HIV-1 and HBV and was associated with a high risk of fibrosis at an odds ratio of 12.6.[22]

Mice with severe combined immunodeficiency disease (SCID) transgenic for the urokinase-type plasminogen activator gene under control of albumin promoter (uPA/SCID mice) have received human hepatocyte transplants.[23-25] These mice [hereafter referred to as chimeric (ChiM) mice] have been instrumental in experiments with hepatitis viruses *in vivo*[26,27] and offer a rare opportunity in portraying the early kinetics of HBV replication,[28] without having to resort to the ever-endangered species of chimpanzees. In this study, ChiM mice were monoinfected with HBV/G or coinfected with other genotypes, either simultaneously or in sequence, and followed for circulating HBV/G DNA. It is hoped that the emerging dynamics of HBV DNA will further characterize the dependence of HBV/G on other genotypes and unfold the pathogenicity intrinsic to this parasitic genotype.

Patients and Methods

Patients. Sera were obtained from 4 patients with chronic hepatitis B. One HBV DNA clone of subgenotype A2 and two of HBV/C2 were recovered from 3 Japanese patients in our recent study.[28] Because all HBV DNA clones of HBV/A were classified into subgenotype A2, they will be called HBV/A comprehensively in the present study. The other HBV/A and G clones were obtained from a coinfected Caucasian patient in San Francisco who represented patient 1 in our previous study.[17] All the HBV/A or C clones did not have precore or core promoter mutations affecting the expression of HBeAg. The study design conformed to the 1975 Declaration of Helsinki and was approved by the institutional ethics committees. Written informed consent was obtained from each patient.

Plasmid Constructs of HBV DNA and Sequencing. HBV DNA was extracted from 100 μL of serum using the QIAamp DNA blood kit (Qiagen, GmbH, Hilden, Germany). Four primer sets were designed for amplification of 2 fragments (A and B) covering the entire HBV/G genome. PCR with nested primers was performed with TaKaRa LA Taq polymerase (Takara Biochemicals, Kyoto, Japan) for 35 cycles (30 s at 95°C; 30 s at 60°C; 2 min at 72°C). Primer pairs and protocols for plasmid construction were described in supporting information. As reported previously,[28] these fragments were constructed into the pUC19 vector deprived of promoters (Invitrogen Corp., Carlsbad, CA) by digestion with *Hin*dIII and *Eco*RI, resulting in 1.24-fold the HBV genome—just enough to transcribe oversized pregenome and precore messenger RNA. Cloned HBV DNA sequences were confirmed with Prism BigDye (Applied Biosystems, Foster City, CA) using the ABI 3100 automated sequencer. Additionally, HBV DNA spanning the complete genome were amplified in mouse sera, cloned in the pGEM-T Easy Vector, and then sequenced.

Cell Culture and Transfection. Huh7 cells were transfected with plasmids equivalent to 5 μg of HBV DNA constructs with use of the Fugene 6 transfection reagent (Roche Diagnostics, Indianapolis, IN), and harvested after 3 days in culture. Transfection efficiency was monitored by 0.5 μg of coinfecting reporter plasmids expressing secreted alkaline phosphatase to estimate the latter's enzymatic activity in the culture supernatant.

Determination of HBV Markers. Hepatitis B surface antigen (HBsAg) and HBeAg were determined via chemiluminescent enzyme immunoassay using commercial assay kits (Fujirebio Inc., Tokyo, Japan). HBV core-related antigens (HBcrAg) were measured in serum using the chemiluminescent enzyme immunoassay described previously.[29,30]

Detection and Quantification of Serum HBV DNA. HBV DNA sequences spanning the S gene were determined via real-time detection PCR according to the method of Abe et al.[31] It had a sensitivity of 100 copies/ml (equivalent to 20 IU/ml) on the assay curve obtained with a calibrated World Health Organization standard serum containing HBV of genotype A (kindly provided by Dr. Hiroshi Yoshizawa of Hiroshima University) when 100 μl of the test sample was used. However, in assays for HBV DNA in mouse sera, in which only 10 μl of sample is used, the sensitivity decreased to 1,000 copies/ml (200 IU/ml). For real-time detection PCR specific for HBV/G, 10 μl of DNA sample was amplified in a 25-μl mixture containing 2 × SYBR Green PCR Master Mix (Applied Biosystems) and 2 primers specific for HBV/G: a forward primer (HBVG1620F: ACG TTA CAT GGA AAC CGC CA) and reverse primer (HBVHKR2: AGC CAA AAA GGC CAT ATG GCA) covering the 36–base pair insertion characteristic of this genotype.[5,16] Amplification and detection were performed in the ABI Prism 7700 Sequence Detection System (Applied Biosystems) with an initial activation of UNG at 50°C for 2 minutes, followed by incubation at 95°C for 10 minutes and subsequently, 40 three-step cycles (30 s at 95°C; 30 s at 60°C; 1 min at 72°C) were performed. The standard was prepared on serial dilutions of a known amount of the cloned HBV plasmid of HBV/G. The specificity of 2 primers (HBVG1620F and HBVHKR2) was confirmed in every PCR run via dissociation curve analysis (ABI Prism 7700 dissociation curve software; Applied Biosystems). The

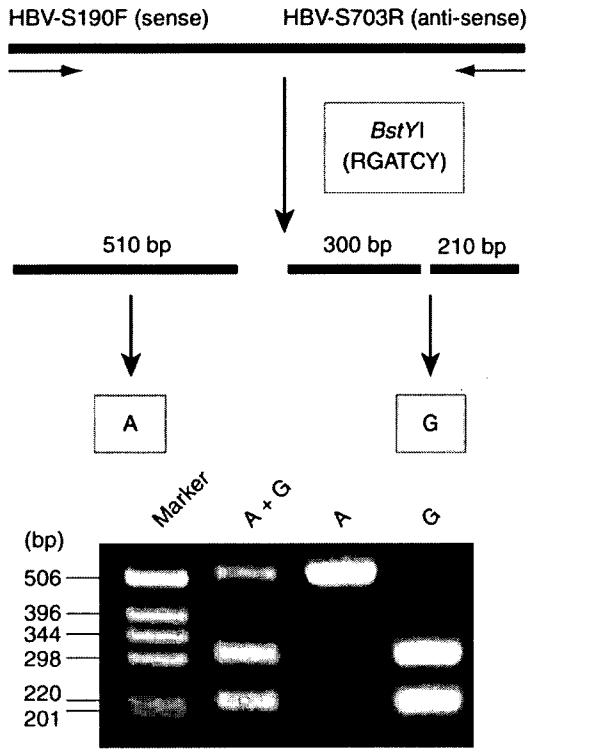

Fig. 1. PCR-RFLP for distinguishing between genotypes A and G. Products of PCR, when digested with *Bst*YI, split into 2 fragments for genotype G (upper panel). Infection with genotype A or G, or coinfection with these genotypes, can be determined by analyzing the patterns of electrophoresis of digests (lower panel).

sensitivity of detecting HBV/G via real-time detection PCR was 1000 copies/ml (200 IU/ml).

PCR Restriction Fragment Length Polymorphism for Distinguishing HBV DNA of Genotype G from Others. A novel method for specific determination of HBV/G DNA in the presence of other genotypes has been developed. It involved single-cycle PCR followed by restriction fragment length polymorphism (RFLP) with an endonuclease having the restriction site specific for HBV/G (Fig. 1). PCR was performed with a forward primer (HBV-S190F: GCT CGT GTT ACA GGC GGG) and reverse primer (HBV-S703R: GAA CCA CTG AAC AAA TGG CAC TAG TA) within the S region. To distinguish HBV/G from other genotypes such as HBV/A and C, a portion (5 μl) of amplification products of 510 base pairs was digested with 5 U *Bst*YI (restriction site: RGATCY) at 60°C for 2 hours. Digests were run on electrophoresis in 3.0% agarose gel, stained with ethidium bromide and examined for their sizes under the ultraviolet light. The results were supported by another method (Supplementary Fig. 1).

Inoculation of Chimeric Mice with the Liver Repopulated for Human Hepatocytes. SCID mice transgenic for the urokinase-type plasminogen activator gene with the liver repopulated for human hepatocytes (chimeric mice) were purchased from Phoenix Bio Co., Ltd. (Hiroshima, Japan). Human serum albumin was measured via ELISA using commercial assay kits (Eiken Chemical Co. Ltd, Tokyo, Japan). They were inoculated with HBV recovered from culture supernatants of Huh7 cells transfected with plasmids constructed with 1.24-fold the HBV genome of genotype HBV/A, C, or G after the method previously reported.[28]

Histopathological Examination. Liver tissues were fixed in buffered formalin, embedded in paraffin, and stained with hematoxylin-eosin or Masson's trichrome. The fibrosis stage was evaluated by an expert pathologist (S. T.) who was blinded to the nature of inocula.

Results

ChiM Mice Monoinfected with HBV/G. Two ChiM mice (ChiM92-3 and ChiM184-4) received an inoculum containing approximately 10^5 copies of HBV/G (G_US1646 strain) and were followed for 12 and 24 weeks, respectively (Fig. 2A,B). HBV DNA remained in undetectable levels ($<10^3$ copies/ml) in them both, but they developed low levels of HBcrAg (1 kU/ml) 4 and 8 weeks after inoculation, respectively. Despite absence of detectable HBV DNA in the circulation, therefore, these mice had contracted infection with HBV/G in very low levels. Intrahepatic cccDNA (covalently closed circular DNA) was detected via PCR specific for it,[32] and HBV/G DNA was detected in hepatocytes via PCR with type-specific primers[33]; they attested to infection with HBV/G in them (data not shown).

Superinfection With HBV/A on Mice Infected with HBV/G. Two chimeric mice with occult infection with HBV/G received 10^5 copies of HBV/A2 of different strains (A2_JPN to ChiM93-4 and A2_USA to ChiM172-3) 10 weeks after initial inoculation with HBV/G (Fig. 3A,B). They both developed HBV DNA in serum in titers $>10^6$ copies/ml at week 17, 7 weeks after superinfection with HBV/A, accompanied by HBcrAg and HBsAg; HBeAg appeared soon thereafter at week 22. HBV DNA and antigens increased, peaked at week 26, and then decreased in exactly the same patterns. HBV/G DNA, which was determined via PCR with type-specific primers, developed 12 weeks after the inoculation at week 22. It increased rapidly, and after the peak, took the same time course as total HBV DNA in serum—it had replaced HBV/A in the two chimeric mice.

Genotypes of HBV in ChiM93-4 were determined at the appearance of HBV DNA (week 17), at peak (week 26), and at the end of observation (week 38) via PCR-

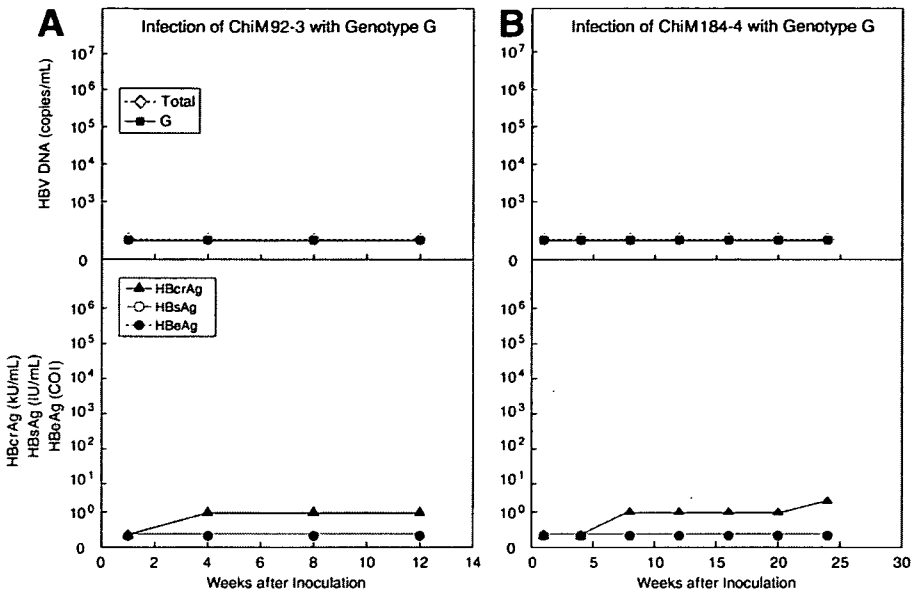

Fig. 2. (A) ChiM92-3 and (B) ChiM184-4 mice monoinfected with HBV/G. Profiles of total HBV DNA and HBV DNA of genotype G, determined via PCR with type-specific primers, are shown in the upper panels, and those of HBV antigens HBVcrAg, HBsAg, and HBeAg are shown in the lower panels. The shaded areas represent HBV DNA titers below the detection limit ($<10^3$ copies/ml).

RFLP (Fig. 3A). HBV/A accounted for all HBV DNA at week 17. At weeks 26 and 38, however, the vast majority of HBV DNA were of HBV/G with a trace of HBV/A. Thus, HBV/G needed coinfection with HBV/A for active replication, and took it over very swiftly.

Superinfection with HVB/G on Mice Infected with HBV/A. The chronological order of superinfection was reversed in ChiM92-9 and ChiM124-11 mice (Fig. 4A,B). The mice received 10^5 copies of HBV/A strains A2_JPN and A2_USA, respectively, and were superinfected with HBV/G (10^5 copies of G_US1646 strain) 10 weeks thereafter, when HBV/A DNA was elevated to $>5 \times 10^7$ copies/ml in both strains. Profiles of HBV DNA and antigens in these mice were quite similar but differed from those with A-on-G superinfection (Fig. 3A,B). HBV/A DNA was detected at week 1 in both groups and increased by approximately 2 logs within the next 3 weeks. HBV/G DNA developed within 3 weeks after superinfection with it, much sooner than the 12 weeks in ChiM mice superinfected with 2 genotypes in the reverse order. Three HBV antigens (HBcrAg, HBsAg, and HBeAg) waxed and waned in profiles similar to that of HBV DNA. HBV DNA levels decreased after they had peaked in ChiM92-9 as in A-on-G mice (Fig. 3A,B) by a margin close to log 2; the decrease was less prominent in ChiM124-11 by merely 1 log.

Composition of different genotypes in serum HBV DNA was followed in ChiM92-9 (Fig. 4A). Rapid replacement of HBV/A with HBV/G was obvious in G-on-A superinfection as in A-on-G superinfection (Fig. 3A). The takeover by HBV/G was not complete as in

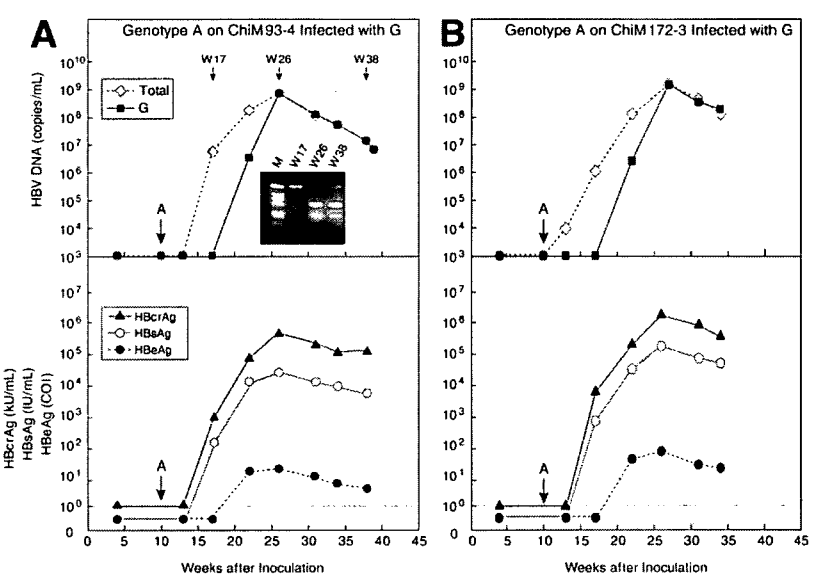

Fig. 3. Superinfection with HBV/A on (A) ChiM93-4 and (B) ChiM172-3 mice infected with HBV/G. Patterns of PCR-RFLP at different time points are shown in the insert in the upper panel of (A). Inoculation with genotype A is indicated by large arrows.

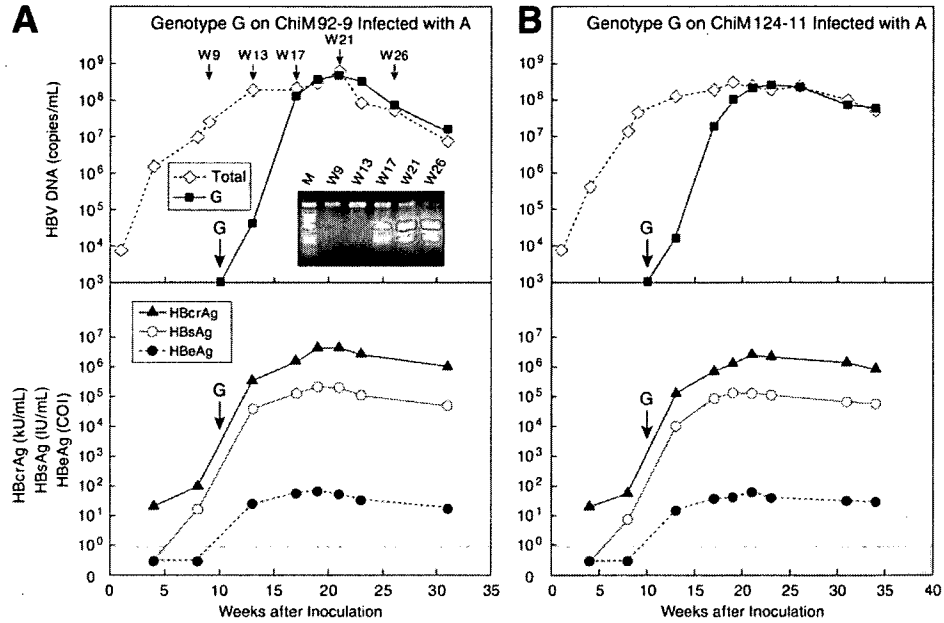

Fig. 4. Superinfection with HBV/G on (A) ChiM92-9 and (B) ChiM124-11 mice infected with HBV/A. Patterns of PCR-RFLP at different time points are shown in the insert in the upper panel of (A). Inoculation with genotype G is indicated by large arrows.

A-on-G superinfection, and HBV/A remained at very low levels throughout the weeks of observation.

Superinfection with HBV/G on Mice Infected with HBV/C. Similar superinfection with HBV/G was performed on ChiM mice that had been infected with HBV/C2 (Fig. 5A,B). Thus, C_22 and C_AT strains (10^5 copies) of HBV/C were injected intravenously into ChiM91-21 and ChiM95-11, respectively. They were superinfected with HBV/G (10^5 copies of G_US1646 strain) at week 10, when HBV DNA stabilized at approximately 10^9 copies/ml. HBV/G appeared in serum 3 weeks thereafter, at week 13 in both groups, and increased exponentially until weeks 21-23. The time required for an increase in HBV DNA level by 10-fold (log time) was 3.3 weeks in both groups, which was twice as long as the 1.6 weeks in mice with A-on-G and G-on-A superinfections (Figs. 3, 4). Likewise, the takeover of HBV/C by HBV/G in these mice was not as rapid or extensive as in superinfection with HBV/G on HBV/A (Figs. 3A, 4A, 5A). HBV antigens took time courses similar to that of HBV DNA, and they never waned after they had stabilized; however, mice were followed until 26 and 34 weeks.

Simultaneous Coinfection of Mice with HBV/A and HBV/G. Two ChiM mice (ChiM93-10 and ChiM93-

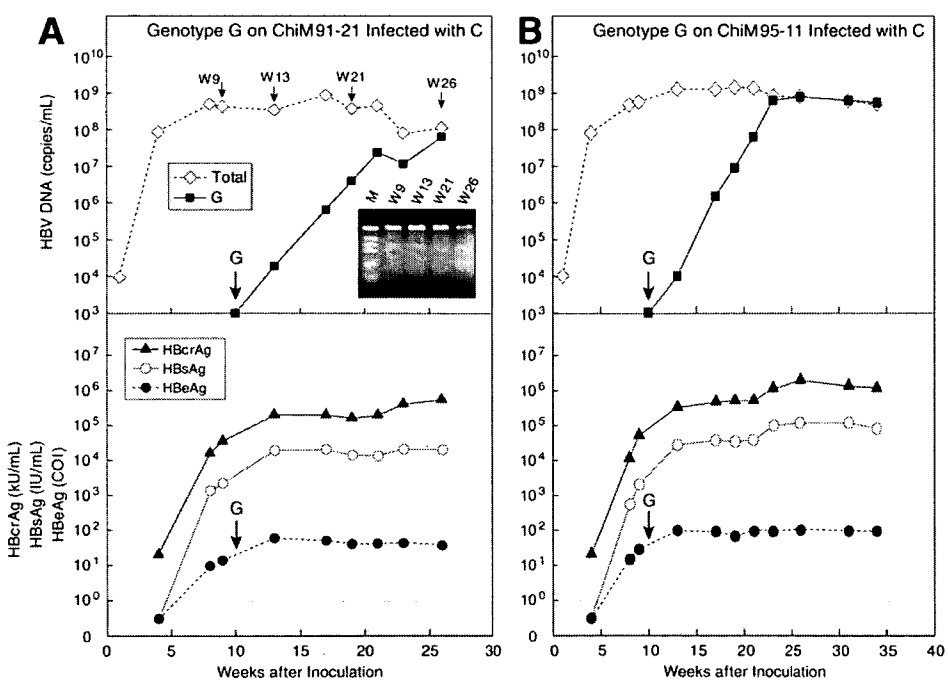

Fig. 5. Superinfection with HBV/G on (A) ChiM91-21 and (B) ChiM95-11 mice infected with HBV/C. Patterns of PCR-RFLP at different time points are shown in the insert the in upper panel of (A). Inoculation with genotype G is indicated by large arrows.

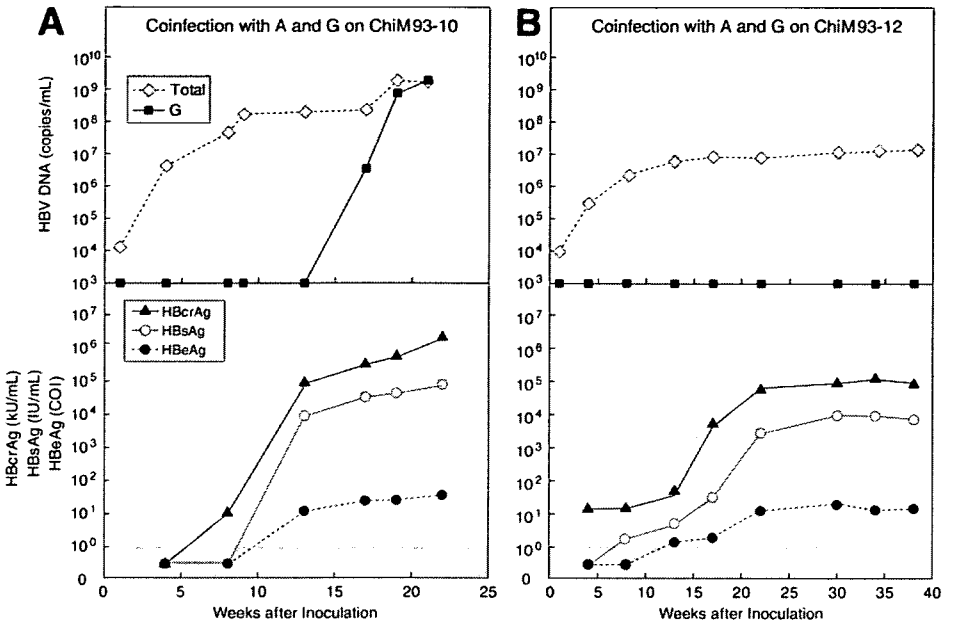

Fig. 6. (A) ChiM93-10 and (B) ChiM93-12 mice simultaneously infected with genotypes A and G.

12) received simultaneous inoculation with 10^5 copies each of HBV/A (A2_JPN strain) and HBV/G (G_US1646 strain). The ChiM93-10 mouse developed HBV/G DNA 17 weeks after inoculation, 9 weeks since HBV/A DNA had increased to $>10^7$ copies/ml (Fig. 6A). HBV/G DNA increased to the level of total HBV DNA at week 21, thereby indicating that by then, HBV/G had taken over HBV/A almost completely.

For the reasons unknown, infection with HBV/G was not established in the ChiM93-12 mouse simultaneously coinfected with HBV/A (Fig. 6B), although it was infected with HBV/A in levels by some 2 logs lower (10^7 copies/ml) than the ChiM93-10 mouse. Serum levels of human albumin in the ChiM93-12 mouse (mean, 2.1×10^6 ng/ml) were much lower than the other chimeric mice used in this study (mean, 4.7×10^6 ng/ml). Thus, a lower extent of repopulation with human hepatocytes may have prohibited active replication of HBV/A. This would be a prerequisite to infection with HBV/G at high levels.

Coinfection of Mice with HBV/A and HBV/G by Inoculation with a Mouse Passage of G-on-A Superinfection. Three ChiM mice (ChiM169-8, ChiM133-3, and ChiM133-6) received serum from a ChiM92-9 mouse with G-on-A superinfection taken at week 26, when HBV/G had almost replaced HBV/A (Fig. 3A). Profiles of HBV/A and HBV/G, after inoculation with 10^5 copies of HBV DNA, were similar among the mice (Fig. 7A-C). HBV/G DNA was detected at week 1 in levels comparable to those of total HBV DNA. Despite receiving the inoculation with a mouse passage containing HBV/G, in copies by 5 logs greater than those of HBV/A, HBV/G DNA decreased thereafter and stayed >1 log lower than total HBV DNA until week 7. Since week 4, HBV/G started to increase and replaced HBV/A almost completely until weeks 10-12, and continued to do so through weeks 19-22 of the observation (Fig. 7A).

Cloning and Sequencing HBV DNA in Chimeric Mice Coinfected with HBV/A and HBV/G. HBV DNA clones from sera of ChiM92-9 sampled at 26 weeks (Fig. 4A) and ChiM169-8 inoculated with serum passage in it (Fig. 7A) included those of HBV/A and G invariably. They confirmed the results of real-time detection PCR and PCR-RFLP and did not possess any mutations in comparison with the original inoculum of either genotype. No recombinations between HBV/A and G were detected, either. At least 5 clones of each genotype were propagated and sequenced in both sera.

Cotransfection of Huh7 Cells with Plasmids Carrying the Core Gene of Genotype A and the Entire Genome of Genotype G. Huh7 cells were transfected with 2 plasmids that were pcDNA_core clones that expressed the core protein of genotype A2, under the control of cytomegalovirus promoter, and the pUC19/G clone incorporated with 1.24-fold the genome of genotype G. Transfection only with genotype G induced its replication in a weak level (Fig. 8). When Huh7 cells were cotransfected with the genotype G clone and the genotype A core clone, however, the replication was enhanced in a dose-dependent manner.

Liver Pathology of ChiM Mice Infected with HBV/A and/or HBV/G. Figure 9 shows the histology of liver in representative ChiM mice either simultaneously coinfected with genotypes A and G (viremia of only ge-

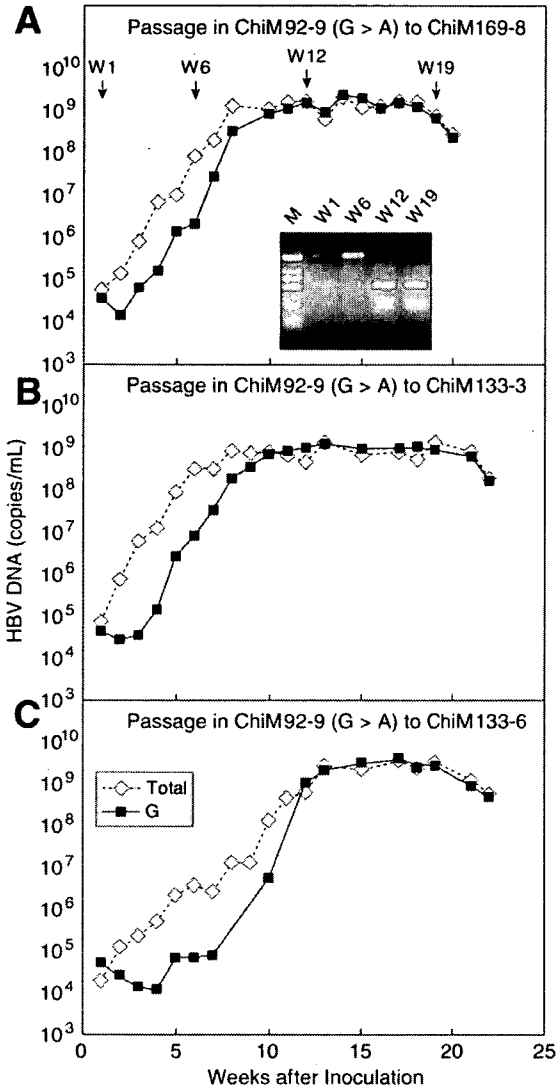

Fig. 7. (A) ChiM169-8, (B) ChiM133-3, and (C) ChiM133-6 mice inoculated with a serum passage from a mouse coinfected with genotypes A and G (ChiM92-9 in Fig. 4A).

notype A in ChiM93-12) or superinfected with genotypes G-on-A (ChiM92-9) and monoinfected with genotype G (ChiM92-3) during 32-39 weeks. HBV infection was demonstrated by double staining for HBcAg and human albumin (Supplementary Fig. 2). The mouse coinfected with genotypes A and G revealed steatosis of hepatocytes with hematoxylin-eosin stain and fibrosis of stage 2 (F2) with Masson's trichrome stain. In contrast, the mice monoinfected with genotype A (ChiM93-12) or G (ChiM92-3) had neither steatosis nor fibrosis. Table 1 summarizes the liver pathology of all autopsied mice. Steatosis in 30%-80% of repopulated human hepatocytes and stage F1-F2 fibrosis were observed in the majority of mice superinfected or coinfected with genotypes G and A or C.

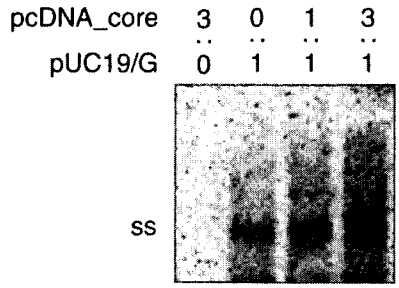

Fig. 8. *Trans*-complementation of the core gene of genotype A for enhanced replication of genotype G. Huh7 cells were cotransfected with plasmids constructed with 1.24-fold the genome of genotype G (pUC19/G) and plasmids expressing the core gene of genotype A (pcDNA_core) in an increasing ratio. Gel strips were Southern-blotted by the complete HBV probe of genotype G. The far left lane represents negative control with pcDNA_core alone. The migration position of single-stranded (ss) HBV DNA is indicated on the left.

Discussion

Using ChiM mice infected with pedigreed HBV DNA in the standardized copy number, we have determined early viral dynamics of HBV/G in detail. Due to constraints on securing ChiM mice with a satisfactory rate of replacement for human hepatocytes (>60%), only 2 or 3 of them were used for each experiment. Concordance of viral dynamics among them, however, would give credence to the reproducibility of obtained results.

HBV/G infected ChiM mice by itself in corroboration with its monoinfection in human beings.[21] The replication was very slow, however, and did not elevate serum HBV DNA to levels detectable by the method used ($>10^3$ copies/ml). Coinfection with HBV/A enhanced the replication of HBV/G remarkably. HBV/G replicated vividly when coinfected with HBV/C, as well. However, the time required for a 10-fold increase (log time) is 2-fold longer in mice initially infected with HBV/C versus HBV/A (3.3 versus 1.6 weeks). Combined, these results would indicate that HBV/G can thrive at the expense of other genotypes, and coinfection with HBV/A is much more advantageous for its enhanced replication than the other genotypes, including HBV/C. In support of this view, coinfection with HBV/A is frequent in individuals infected with HBV/G.[16,34] Such a heavy dependence of HBV/G on HBV/A does not require recombination between them, because no recombination events occurred in ChiM mice coinfected with them.

The initial replication of HBV/G was much slower than that of HBV/A, even in simultaneous coinfection. This was typically observed in three ChiM mice inoculated with a mouse passage of G-on-A superinfection containing HBV/G in the concentration a few logs higher than that of HBV/A. Despite such an enormous difference in introduced virions, the replication of HBV/A far

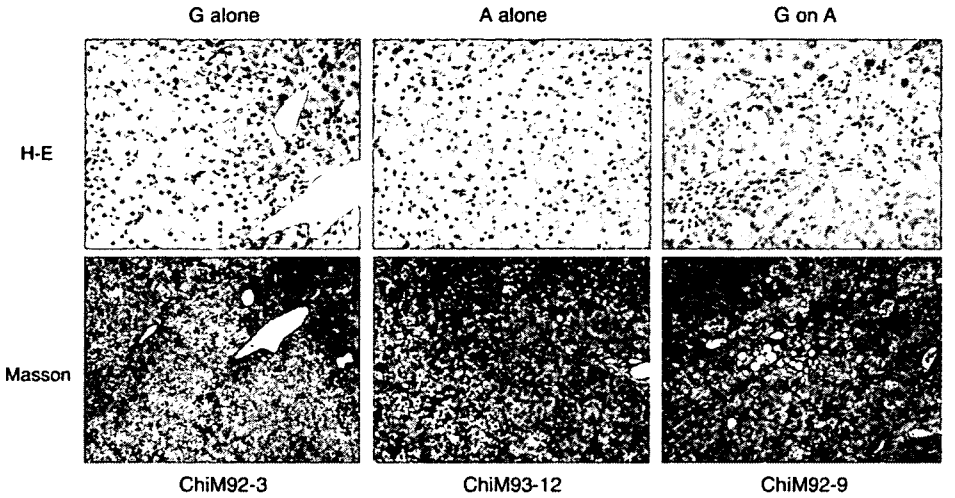

Fig. 9. Liver histology in a ChiM92-3 mouse monoinfected with genotype G, a ChiM93-12 mouse coinfected with genotypes A and G (but persistently infected with genotype A alone), and a ChiM92-9 mouse superinfected with genotype G-on-A. Liver sections stained with hematoxylin-eosin or Masson's trichrome stain are shown.

exceeded that of HBV/G in the initial several weeks. Thereafter, HBV/G caught up with HBV/A, then took it over almost completely. Such a replacement was observed when HBV/G was superinfected on HBV/A, or vice versa.

The mechanism by which genotype G depends on genotype A for replication was pursued in cotransfection experiments in Huh7 cells. Cotransfection with the pcDNA_core clone carrying the core gene of genotype A2 increased the replication of the pUC19/G clone constructed with 1.24-fold the genome of genotype G in a dose-dependent manner (Fig. 8). Hence, *trans*-complementation with the core protein of genotype A would be required for genotype G to replicate actively. The possibility remains, however, for other viral elements from coinfecting genotypes to enhance the replication of genotype G. Cotransfection of cultured cells with genotype G and others would help clarify how it depends on coinfecting the other genotypes.[35]

Table 1. Steatosis and Fibrosis in Human Hepatocytes in the Liver of Chimeric Mice Monoinfected or Coinfected with HBV/G

		Features	
Inoculation	Mouse No.	Steatosis (%)*	Fibrosis Stage
G alone	ChiM92-3	<5	F0
	ChiM 184-4	<5	F0
A alone	ChiM 93-12†	<5	F0
A-on-G	ChiM 93-4	50	F1
	ChiM 172-3	40	F1
G-on-A	ChiM 92-9	40	F2
	ChiM 124-11	50	F1
G-on-C	ChiM 91-21	80	F2
	ChiM 95-11	NA	NA
A plus G	ChiM 93-10	30	F0
Passage	ChiM 169-8	50	F1
A plus G	ChiM 133-3	<5	F2
	ChiM 133-6	30	F2

Abbreviation: NA, not available.

*Percentage of human hepatocytes with steatosis. †Simultaneously inoculated with A plus G but became infected with genotype A only (Fig. 6B).

Coinfection with HBV/G may be associated with pathological manifestations. ChiM mice coinfected with HBV/A and HBV/G developed steatosis and fibrosis in the liver not observed in mice monoinfected with either of these genotypes. Very recently, Lacombe et al.[22] reported more severe fibrosis in HIV-positive French patients who were infected with HBV/G than the others; they would most likely have been coinfected with other genotypes in undetectable levels. On the basis of clinical and experimental pieces of evidence, it does seem that HBV/G has a strong disease-inducing capacity, which would be operable only when it is coinfected with other genotypes. High levels of HBcrAg in mice with HBV/G (Figs. 3-6) under immunocompromised states would implicate accumulation of the product of the core gene in the fibrosis of patients coinfected with it and HIV. Patients with HIV are infected with HBV at a frequency of 6%-9%, and liver-related deaths happen more often in coinfected patients.[36,37] Fibrosis proceeds faster in patients coinfected with HIV and HBV, as in those with HCV.[38,39] Therapeutic intervention to prevent fibrosis would be required in patients coinfected with HIV and HBV, particularly in HBV/G patients.

In conclusion, the early viral dynamics of HBV/G have been characterized in ChiM mice monoinfected with HBV/G or coinfected with other genotypes. The replication of HBV/G is very slow and depends heavily on coinfection with other genotypes. HBV/G rapidly takes over

the other genotypes, though they are indispensable. Infection with HBV/G may induce steatosis and fibrosis in the liver—but again, only in the case of coinfection with other genotypes. However, it is still unclear whether or not such an increased pathogenicity of HBV/G is expressed exclusively in animals and patients with genetic or acquired immune deficiency.

References

1. Lee WM. Hepatitis B virus infection. N Engl J Med 1997;337:1733-1745.
2. Arauz-Ruiz P, Norder H, Robertson BH, Magnius LO. Genotype H: a new Amerindian genotype of hepatitis B virus revealed in Central America. J Gen Virol 2002;83:2059-2073.
3. Norder H, Hammas B, Lofdahl S, Courouce AM, Magnius LO. Comparison of the amino acid sequences of nine different serotypes of hepatitis B surface antigen and genomic classification of the corresponding hepatitis B virus strains. J Gen Virol 1992;73:1201-1208.
4. Okamoto H, Tsuda F, Sakugawa H, Sastrosoewignjo RI, Imai M, Miyakawa Y, et al. Typing hepatitis B virus by homology in nucleotide sequence: comparison of surface antigen subtypes. J Gen Virol 1988;69: 2575-2583.
5. Stuyver L, De Gendt S, Van Geyt C, Zoulim F, Fried M, Schinazi RF, et al. A new genotype of hepatitis B virus: complete genome and phylogenetic relatedness. J Gen Virol 2000;81:67-74.
6. Naumann H, Schaefer S, Yoshida CF, Gaspar AM, Repp R, Gerlich WH. Identification of a new hepatitis B virus (HBV) genotype from Brazil that expresses HBV surface antigen subtype adw4. J Gen Virol 1993;74:1627-1632.
7. Miyakawa Y, Mizokami M. Classifying hepatitis B virus genotypes. Intervirology 2003;46:329-338.
8. Schaefer S. Hepatitis B virus: significance of genotypes. J Viral Hepat 2005;12:111-124.
9. Chu CJ, Lok AS. Clinical significance of hepatitis B virus genotypes. HEPATOLOGY 2002;35:1274-1276.
10. Liu CJ, Kao JH, Chen DS. Therapeutic implications of hepatitis B virus genotypes. Liver Int 2005;25:1097-1107.
11. Sugauchi F, Kumada H, Sakugawa H, Komatsu M, Niitsuma H, Watanabe H, et al. Two subtypes of genotype B (Ba and Bj) of hepatitis B virus in Japan. Clin Infect Dis 2004;38:1222-1228.
12. Tanaka Y, Orito E, Yuen MF, Mukaide M, Sugauchi F, Ito K, et al. Two subtypes (subgenotypes) of hepatitis B virus genotype C: A novel subtyping assay based on restriction fragment length polymorphism. Hepatol Res 2005;33:216-224.
13. Sugauchi F, Kumada H, Acharya SA, Shrestha SM, Gamutan MT, Khan M, et al. Epidemiological and sequence differences between two subtypes (Ae and Aa) of hepatitis B virus genotype A. J Gen Virol 2004;85:811-820.
14. Akuta N, Suzuki F, Kobayashi M, Tsubota A, Suzuki Y, Hosaka T, et al. The influence of hepatitis B virus genotype on the development of lamivudine resistance during long-term treatment. J Hepatol 2003;38:315-321.
15. Tanaka Y, Hasegawa I, Kato T, Orito E, Hirashima N, Acharya SK, et al. A case-control study for differences among hepatitis B virus infections of genotypes A (subtypes Aa and Ae) and D. HEPATOLOGY 2004;40:747-755.
16. Kato H, Orito E, Gish RG, Sugauchi F, Suzuki S, Ueda R, et al. Characteristics of hepatitis B virus isolates of genotype G and their phylogenetic differences from the other six genotypes (A through F). J Virol 2002;76:6131-6137.
17. Kato H, Orito E, Gish RG, Bzowej N, Newsom M, Sugauchi F, et al. Hepatitis B e antigen in sera from individuals infected with hepatitis B virus of genotype G. HEPATOLOGY 2002;35:922-929.
18. Perez-Olmeda M, Nunez M, Garcia-Samaniego J, Rios P, Gonzalez-Lahoz J, Soriano V. Distribution of hepatitis B virus genotypes in HIV-infected patients with chronic hepatitis B: therapeutic implications. AIDS Res Hum Retroviruses 2003;19:657-659.
19. Suwannakarn K, Tangkijvanich P, Theamboonlers A, Abe K, Poovorawan Y. A novel recombinant of hepatitis B virus genotypes G and C isolated from a Thai patient with hepatocellular carcinoma. J Gen Virol 2005;86:3027-3030.
20. Sanchez LV, Tanaka Y, Maldonado M, Mizokami M, Panduro A. Difference of hepatitis B virus genotype distribution in two groups of Mexican patients with different risk factors. High prevalence of genotype H and G. Intervirology 2007;50:9-15.
21. Chudy M, Schmidt M, Czudai V, Scheiblauer H, Nick S, Mosebach M, et al. Hepatitis B virus genotype G monoinfection and its transmission by blood components. HEPATOLOGY 2006;44:99-107.
22. Lacombe K, Massari V, Girard PM, Serfaty L, Gozlan J, Pialoux G, et al. Major role of hepatitis B genotypes in liver fibrosis during coinfection with HIV. AIDS 2006;20:419-427.
23. Heckel JL, Sandgren EP, Degen JL, Palmiter RD, Brinster RL. Neonatal bleeding in transgenic mice expressing urokinase-type plasminogen activator. Cell 1990;62:447-456.
24. Rhim JA, Sandgren EP, Degen JL, Palmiter RD, Brinster RL. Replacement of diseased mouse liver by hepatic cell transplantation. Science 1994; 263:1149-1152.
25. Tateno C, Yoshizane Y, Saito N, Kataoka M, Utoh R, Yamasaki C, et al. Near completely humanized liver in mice shows human-type metabolic responses to drugs. Am J Pathol 2004;165:901-912.
26. Mercer DF, Schiller DE, Elliott JF, Douglas DN, Hao C, Rinfret A, et al. Hepatitis C virus replication in mice with chimeric human livers. Nat Med 2001;7:927-933.
27. Tsuge M, Hiraga N, Takaishi H, Noguchi C, Oga H, Imamura M, et al. Infection of human hepatocyte chimeric mouse with genetically engineered hepatitis B virus. HEPATOLOGY 2005;42:1046-1054.
28. Sugiyama M, Tanaka Y, Kato T, Orito E, Ito K, Acharya SK, et al. Influence of hepatitis B virus genotypes on the intra- and extracellular expression of viral DNA and antigens. HEPATOLOGY 2006;44:915-924.
29. Kimura T, Ohno N, Terada N, Rokuhara A, Matsumoto A, Yagi S, et al. Hepatitis B virus DNA-negative dane particles lack core protein but contain a 22-kDa precore protein without C-terminal arginine-rich domain. J Biol Chem 2005;280:21713-21719.
30. Shinkai N, Tanaka Y, Orito E, Ito K, Ohno T, Hirashima N, et al. Measurement of hepatitis B virus core-related antigen as predicting factor for relapse after cessation of lamivudine therapy for chronic hepatitis B virus infection. Hepatol Res 2006;36:272-276.
31. Abe A, Inoue K, Tanaka T, Kato J, Kajiyama N, Kawaguchi R, et al. Quantitation of hepatitis B virus genomic DNA by real-time detection PCR. J Clin Microbiol 1999;37:2899-2903.
32. Mason AL, Xu L, Guo L, Kuhns M, Perrillo RP. Molecular basis for persistent hepatitis B virus infection in the liver after clearance of serum hepatitis B surface antigen. HEPATOLOGY 1998;27:1736-1742.
33. Kato H, Orito E, Sugauchi F, Ueda R, Gish RG, Usuda S, et al. Determination of hepatitis B virus genotype G by polymerase chain reaction with hemi-nested primers. J Virol Methods 2001;98:153-159.
34. Osiowy C, Giles E. Evaluation of the INNO-LiPA HBV genotyping assay for determination of hepatitis B virus genotype. J Clin Microbiol 2003;41: 5473-5477.
35. Kremsdorf D, Garreau F, Capel F, Petit MA, Brechot C. In vivo selection of a hepatitis B virus mutant with abnormal viral protein expression. J Gen Virol 1996;77:929-939.
36. Konopnicki D, Mocroft A, de Wit S, Antunes F, Ledergerber B, Katlama C, et al. Hepatitis B and HIV: prevalence, AIDS progression, response to highly active antiretroviral therapy and increased mortality in the EuroSIDA cohort. AIDS 2005;19:593-601.
37. Thio CL, Seaberg EC, Skolasky R Jr, Phair J, Visscher B, Munoz A, et al. HIV-1, hepatitis B virus, and risk of liver-related mortality in the Multicenter Cohort Study (MACS). Lancet 2002;360:1921-1926.
38. Benhamou Y, Bochet M, Di Martino V, Charlotte F, Azria F, Coutellier A, et al. Liver fibrosis progression in human immunodeficiency virus and hepatitis C virus coinfected patients. The Multivirc Group. HEPATOLOGY 1999;30:1054-1058.
39. Colin JF, Cazals-Hatem D, Loriot MA, Martinot-Peignoux M, Pham BN, Auperin A, et al. Influence of human immunodeficiency virus infection on chronic hepatitis B in homosexual men. HEPATOLOGY 1999;29:1306-1310.

Chemistry & Biology
Article

Synthesis of Polyester by Means of Genetic Code Reprogramming

Atsushi Ohta,[1] Hiroshi Murakami,[2] Eri Higashimura,[1] and Hiroaki Suga[1,2,*]
[1]Department of Chemistry and Biotechnology, Graduate School of Engineering, The University of Tokyo, 113-8656 Tokyo, Japan
[2]Research Center for Advanced Science and Technology, The University of Tokyo, 153-8904 Tokyo, Japan
*Correspondence: hsuga@rcast.u-tokyo.ac.jp
DOI 10.1016/j.chembiol.2007.10.015

SUMMARY

Here we report the ribosomal polymerization of α-hydroxy acids by means of genetic code reprogramming. The flexizyme system, a ribozyme-based tRNA acylation tool, was used to reassign individual codons to seven types of α-hydroxy acids, and then polyesters were synthesized under controls of the reprogrammed genetic code using a reconstituted cell-free translation system. The sequence and length of the polyester segments were specified by the mRNA template, indicating that high-fidelity ribosome expression of polyesters was possible. This work opens a door for the mRNA-directed synthesis of backbone-altered biopolymers.

INTRODUCTION

The translation system polymerizes amino acids to polypeptides using the genetic information present in the form of trinucleotide codons in the mRNA sequences. In this manner, the ribosome machinery acts as a template-directed synthesizer of polymers consisting of amino acids. Each of the codons directs the incorporation of 1 of 20 proteinogenic α-amino acids into the polypeptide chain, and therefore the ribosome is generally used for the synthesis of polypeptides, not for other biopolymers. If the codons are reassigned to nonproteinogenic amino acids, and if the translation system is adaptable to such alterations, mRNA-directed synthesis of nonproteogenic polypeptides by means of genetic code reprogramming is possible [1–6]. However, we have not yet witnessed the ribosomal synthesis of biopolymers with a nonpeptide backbone by such a methodology.

An α-hydroxy acid is chemically analogous to an α-amino acid, where the hydroxy group acts as a nucleophile. Despite this atomic difference, the ribosome is able to accept an α-hydroxy acid as a substrate to form an ester bond when hydroxyacyl-tRNA (ha-tRNA) is supplied to the translation system [7–14]. Previously, the specific incorporation of a single α-hydroxy acid into the polypeptide chain using amber stop codon suppression has been reported [7, 8, 10, 13]. Unfortunately, this strategy allows for the assignment of only a single kind of α-hydroxy acid, and therefore it is not suitable for the synthesis of complex polyesters composed of several different α-hydroxy acids.

In another approach reported over 30 years ago, the ribosome polymerizes phenyllactic acid (F^{lac}) on polyuridylic acid (poly-U) via random initiation and termination upon the addition of F^{lac}-$tRNA^{Phe}$ [12]. However, due to the methodology for the preparation of F^{lac}-$tRNA^{Phe}$ where Phe-$tRNA^{Phe}$ was chemically deaminated by nitrous acid, it was difficult to deplete the Phe-$tRNA^{Phe}$ contaminant completely from the translation mixture; therefore, the resulting polyester was actually composed of a heterogeneous random mixture of F^{lac} and Phe with a ratio of approximately 7:3. Due to the fact that the poly-U template did not specify either a start or stop site, the ribosome could randomly initiate or terminate the synthesis of polyesters, and thus the length of the synthesized polyester could not be regulated.

Collectively, these previous findings indicate that the ribosome is capable of catalyzing the polymerization of α-hydroxy acids, but it remains unknown whether the mRNA-directed polymerization of several different α-hydroxy acids is possible. Here we report the synthesis of polyester composed of various α-hydroxy acids using a reprogrammed genetic code where the codons are reassigned from proteinogenic α-amino acids to α-hydroxy acids.

RESULTS

Genetic Code Reprogramming for the Incorporation of α-Hydroxy Acids

To demonstrate programmed synthesis of polyesters, we took advantage of two recently developed technologies (Figure 1). The first one is a de novo tRNA acylation system consisting of artificially evolved ribozymes, called flexizymes [14–17]. This system enables us to charge various hydroxy acids onto tRNAs bearing any desired anticodons and body sequences. The second one is a reconstituted *Escherichia coli* cell-free translation system, called the PURE (protein synthesis using recombinant elements) system [18, 19]. This translation system lets us create vacant codon boxes by withdrawing the corresponding aminoacyl-tRNA synthetases (ARSs) and amino acids from the reconstituted translation mixture (referred to as

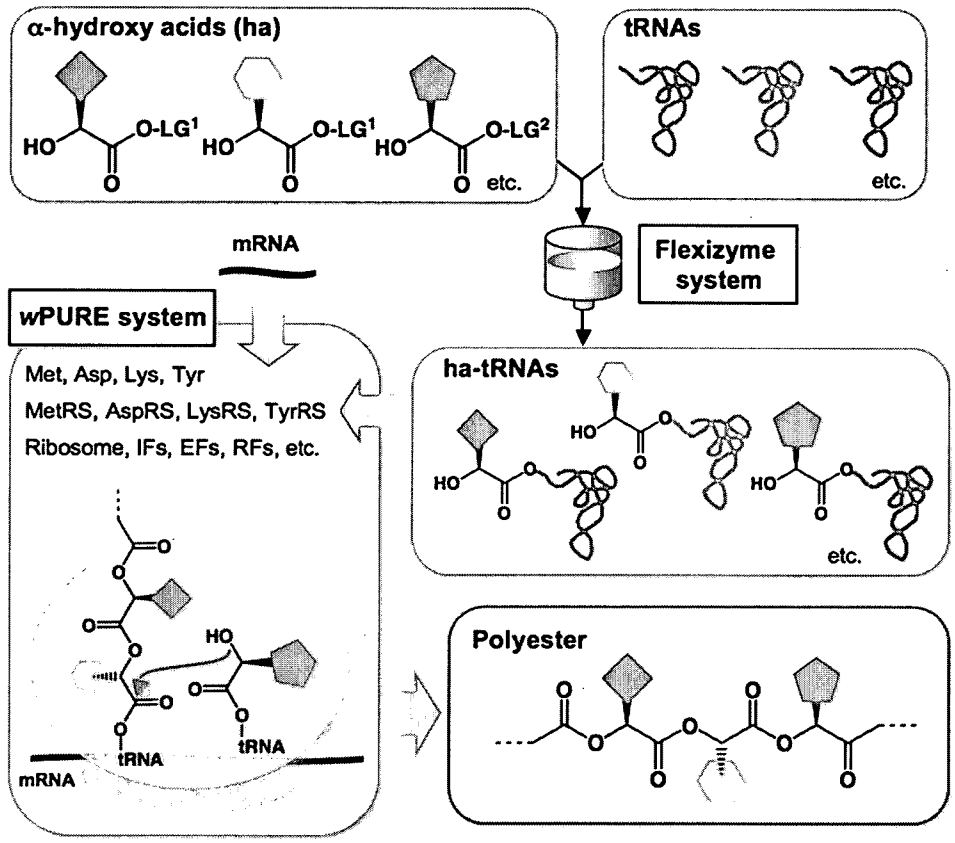

Figure 1. Ribosomal Polyester Synthesis by Means of the Flexizyme (eFlexiresin or dFlexiresin) and *w*PURE Systems
LG^1 and LG^2 indicate cyanomethyl and 3,5-dinitrobenzyl leaving groups, respectively (see Figure 2A). IFs, initiation factors; EFs, elongation factors; RFs, release factors.

the *w*PURE system). Vacant codons can then be reassigned to any desired α-hydroxy acids by using the flexizyme system to charge the α-hydroxy acids to the vacant codon's cognate tRNA. By combining these two technologies, the genetic code can be reprogrammed for the mRNA-directed synthesis of polyesters.

We chose seven α-hydroxy acids, of which four were phenyllactic acid derivatives (F^{lac}, mF^{lac}, and cF^{lac}, pF^{lac}) and three were nonaromatic α-hydroxy acids (G^{lac}, L^{lac}, and A^{lac}), to investigate mRNA template-directed ester polymerization (Figure 2A). We arbitrarily selected seven codons, and their corresponding anticodons were implanted into $tRNA^{Asn\text{-}E1}_{NNN}$ and $tRNA^{Asn\text{-}E2}_{NNN}$ sequences (NNN indicates anticodon sequence; Figures 3A and 3B), with each of the seven codons assigned to one of the seven α-hydroxy acids (Figure 2B). These tRNA sequences were chosen because we have previously shown that they could act as orthogonal tRNAs in the PURE system [14]. We next designed the mRNA template to initiate the polyester synthesis with fMet. For purification and detection purposes, we also incorporated a modified FLAG peptide (KKDYKDDDDK) at the C terminus (vide infra). Accordingly, the *w*PURE system for the polyester synthesis included only four amino acids (Met [M], Lys [K], Asp [D], and Tyr [Y]) and their cognate ARSs. It should be noted that although the translated polyesters would be conjugated with the above polypeptide sequence (i.e., polyester-polypeptide hybrids would be translated), the polypeptide segment was embedded in the polymers strictly for detection and purification purposes. Because the genetic code reprogramming was applied to the polyester segments only, we referred to such polymers as polyesters for the sake of simplicity of our experimental significance.

We first tested whether each tRNA bearing the designated anticodon retained its orthogonality and thereby could incorporate an α-hydroxy acid at a single template-directed position in a model polypeptide, without significant competition from other amino acids present in the translation mixture. Our conventional assay using a microhelix RNA indicated that the flexizyme system was able to efficiently charge all of the α-hydroxy acids onto either $tRNA^{Asn\text{-}E1}_{NNN}$ or $tRNA^{Asn\text{-}E2}_{NNN}$ (see Figure S1 in the Supplemental Data available with this article online). All of the α-hydroxy acid-charged tRNAs retained their orthogonality in the *w*PURE system, unfortunately with one exception: neither $tRNA^{Asn\text{-}E1}_{CUG}$ nor $tRNA^{Asn\text{-}E2}_{CUG}$ bearing a CUG anticodon assigning A^{lac} possessed the expected orthogonality, resulting in the minor incorporation of Lys into the targeted CAG position in the

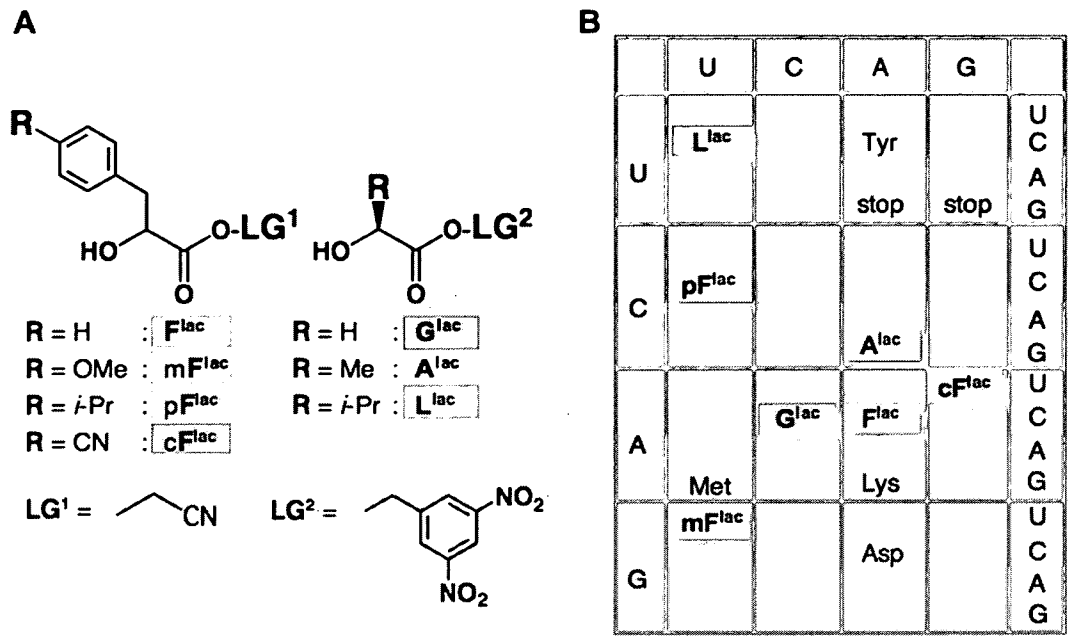

Figure 2. Genetic Code Reprogramming for mRNA-Directed Polyester Synthesis

(A) Chemical structure and abbreviation of α-hydroxy acids used in this study. F^{lac}, phenyllactic acid; mF^{lac}, *p*-methoxyphenyllactic acid; pF^{lac}, *p*-isopropylphenyllactic acid; cF^{lac}, *p*-cyanophenyllactic acid; G^{lac}, glycolic acid; A^{lac}, lactic acid; L^{lac}, isopropyllactic acid. The abbreviations used are based on structurally similar amino acids. The stereochemistry of pF^{lac}, mF^{lac}, and cF^{lac} is racemic, whereas that of other α-hydroxy acids is *S* configuration. All phenyllactic acid derivatives bear a cyanomethyl ester group (LG^1) and are charged onto tRNAs shown in Figure 3 using eFlexiresin, while others bear a 3,5-dinitrobenzyl ester group (LG^2) and are charged onto the tRNAs using dFlexiresin.

(B) The reprogrammed genetic code used in this study. α-hydroxy acids assigned to the respective triplets are color-coded as shown.

polyester-reading frame. Presumably, these tRNAs were susceptible to Lys misacylation by LysRS included in the *w*PURE system, so that the resulting Lys-$tRNA^{Asn\text{-}E1/E2}_{CUG}$ competed with the A^{lac}-$tRNA^{Asn\text{-}E1/E2}_{CUG}$ for incorporation into the polypeptide chain (data not shown). To circumvent this problem, we developed an orthogonal tRNA derived from a *Mycobacteriophage L5* $tRNA^{Asn}_{CUG}$ ($tRNA^{MLAsn}$ in Figure 3C). We found that $tRNA^{MLAsn}_{CUG}$ was not aminoacylated with Lys by LysRS, and thus the misincorporation of Lys was not observed. To this end, we engineered each of the seven anticodons, each assigned to a different α-hydroxy acid, into three different tRNA body sequences to explore the mRNA-directed expression of polyesters (Figures 2B and 3A–3C).

mRNA-Directed Synthesis of Polyesters Containing Four Consecutive Ester Linkages

We designed four nucleotide templates (hereafter referred to as T1–T4) to express polyesters (E1–E4) consisting of four consecutive ester bonds in the *w*PURE system (Figure 4A). As a control, these templates were also translated in the conventional PURE system, and thereby the expression level of polyesters could be compared with that of polypeptides (P1–P4). To detect the expressed products containing polyester, [^{14}C]Asp was included in the *w*PURE system. [^{14}C]Asp was incorporated into the Asp residues in the C-terminal FLAG peptide sequence, and the expressed polyester-[^{14}C]FLAG products were monitored by tricine-SDS-PAGE and autoradiography.

Tricine-SDS-PAGE analysis revealed that expression of E1 was observed only when all ha-tRNAs were present in the *w*PURE system and its expression level was comparable to that of the control peptide, P1 (Figure 4B, lanes 1–5). The molecular mass (ms) of E1 determined by MALDI-TOF analysis was consistent with the calculated ms of the full-length E1 (Figure 5A, E1). Likewise, the respective T2–T4 templates expressed the E2–E4 polyesters with the expected ms (Figure 4B, lanes 6–11; Figure 5A, E2–E4). The expression levels of P1, E1, E2, E3, and E4 were estimated by the incorporation of [^{14}C]Asp by tricine-SDS-PAGE autoradiography analysis considering that five aspartic acids were included in the polymers, giving approximately 6 pmol/5 μl, 9.5 pmol/5 μl, 15 pmol/5 μl, 12 pmol/5 μl, and 5.3 pmol/5 μl, respectively (data not shown). These results provide solid evidence that the length and sequence of the tetrapolyesters are strictly controlled by the mRNA template sequence.

mRNA-Directed Synthesis of Longer Polyesters

We next explored the capability of ribosomes for the synthesis of various lengths of polyesters. In addition to T1 expressing tetrapolyester E1, five templates T5–T9 were designed to express tri-, penta-, hexa-, octa-, and dodecapolyesters E5–E9 (Figure 4A). We were able to detect tripolyester E5 with the expected ms similar to that of tetrapolyester E1 (Figure 5B, E5 and E1), whereas the full-length peak of pentapolyester E6 was barely detectable exhibiting a significantly poor signal/noise ratio, while the

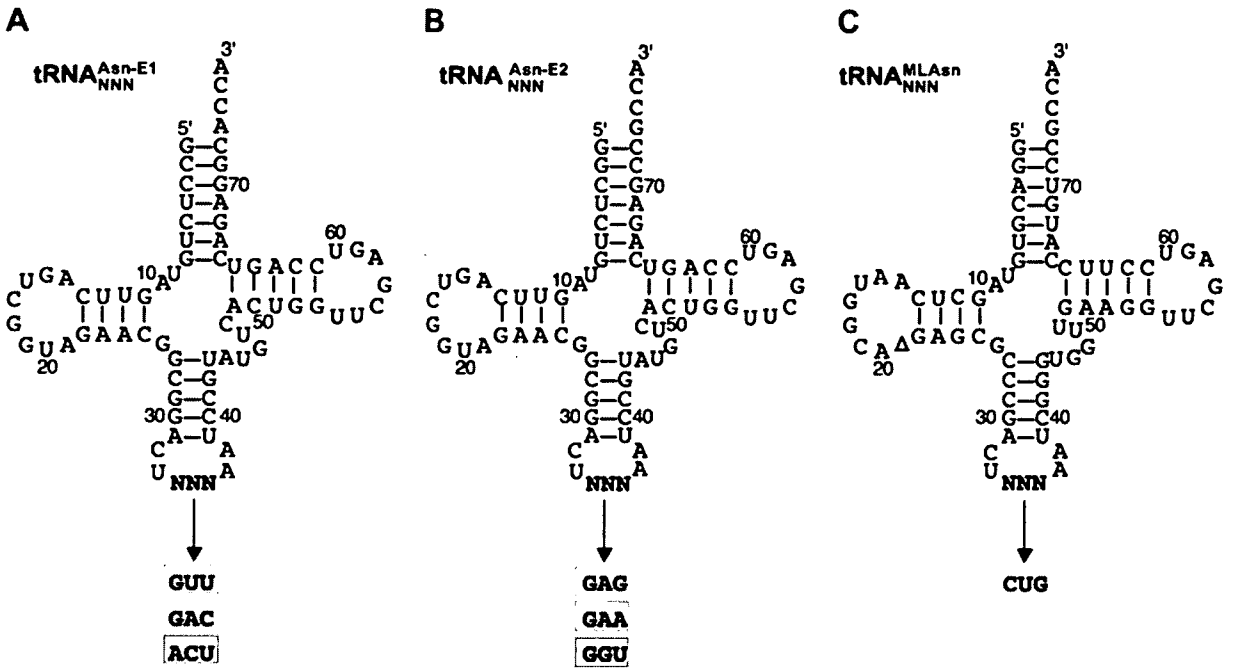

Figure 3. Three tRNA Body Sequences Used in This Study
(A) $tRNA^{Asn\text{-}E1}_{NNN}$.
(B) $tRNA^{Asn\text{-}E2}_{NNN}$.
(C) $tRNA^{MLAsn}_{NNN}$. NNN indicates anticodon and each anticodon is color-coded to pair with the corresponding codon shown in Figure 2B.

full-length peaks of E7–E9 were not detected (Figure S2). We wondered whether the lack of a full-length peak of E7–E9 was due to a significant reduction in polyester expression. Tricine-SDS-PAGE analysis showed that the expression level was slightly diminished as the polyester became longer, yet a detectable level of expression was observed for E6–E9 (Figure 4B, lanes 12–19). Due to the fact that [^{14}C]Asp was incorporated into the C-terminal FLAG sequence, we concluded that the polyester-FLAG could be expressed in all cases. We thus speculated that the full-length E6–E9 might be difficult to ionize under ordinary MALDI-TOF conditions. Unfortunately, attempts under more stringent ionization conditions, such as longer/stronger irradiation or the use of other matrices, resulted in fragmentation of the polyesters (data not shown).

Due to the difficulty in ionization of polyesters longer than a pentapolyester, we modified the strategy to obtain evidence for longer polyesters by MALDI-TOF analysis. The full-length polyester was hydrolyzed under basic conditions to generate shortened fragments. Because the FLAG peptide region could not be hydrolyzed under such conditions, we expected that $(ha)_n$-FLAG (n indicates the number of α-hydroxy acyl groups [ha] remaining after the base hydrolysis) could be detected by MALDI-TOF. Indeed, upon analysis of the hydrolyzed products, we were able to observe the $(ha)_2$-FLAG product as a major peak for E6–E9, occasionally with a minor peak of ha-FLAG (Figure 5B, E6–E9). Most importantly, the observed ms for each of the $(ha)_2$-FLAG products hydrolytically generated from the full-length E6–E9 was consistent with the expected ms of $(ha)_2$-FLAG encoded by the respective mRNA sequence (Figure 4A). Taken together, our findings show that polyesters can be continuously synthesized up to dodecapolyester in accordance with the mRNA template.

DISCUSSION

The flexizyme system is a highly flexible acylation tool that enables us to charge various acids onto any desired tRNAs. By means of this system, we were able to readily prepare tRNAs charged with a variety of α-hydroxy acids (ha-tRNAs). The various ha-tRNAs were then utilized in a special reconstituted cell-free translation system in which unneeded amino acids and their corresponding ARSs are withdrawn from the translation mixture (referred to as the *w*PURE system). Removal of such components creates vacant codons which can then be reassigned to specific α-hydroxy acids using the flexizyme system to generate ha-tRNAs that designate the respective codons. Thus, by combining these two technologies, we could use ribosomes for the synthesis of mRNA template-designed polyesters. Our data clearly show that polyesters of up to 12 α-hydroxy acids in length could be synthesized with the length and sequence defined by the mRNA template.

Currently, it is not clear what hindered the synthesis of polyesters longer than 12 α-hydroxy acids, yet based on this study and our other unpublished work on the incorporation of exotic amino acids into the nascent peptide

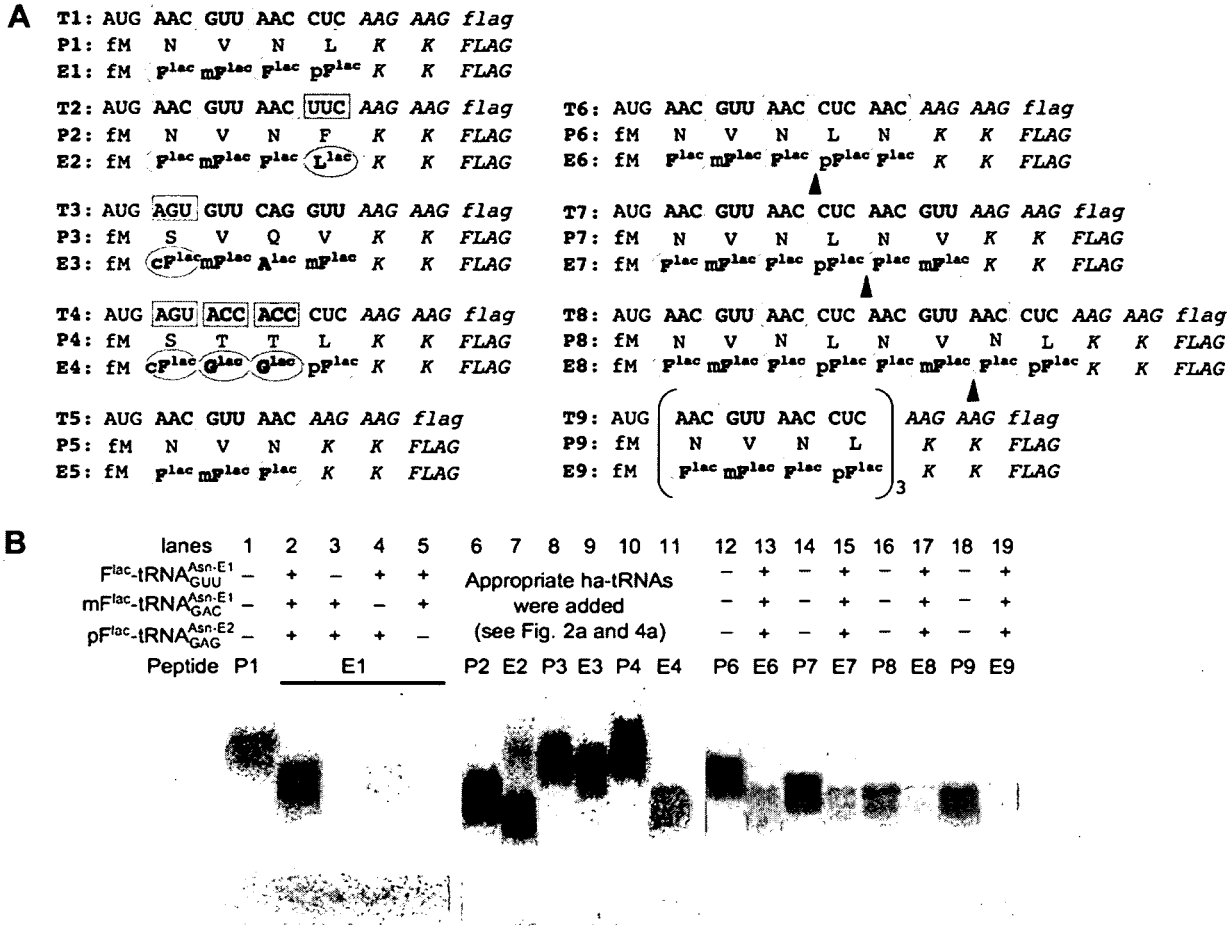

Figure 4. Polyester Synthesis

(A) Sequences of mRNA templates (T1–T9), polypeptides (P1–P9), and polyesters (E1–E9). Reprogrammed codons in mRNA (rectangles) and α-hydroxy acids (circles) are highlighted in colors matching those in Figure 2B. Black arrowheads indicate the positions of hydrolyzed ester bonds that give $(ha)_2$-FLAGs observed in Figure 5B.

(B) Tricine-SDS-PAGE analysis of the expressed products. The products, labeled with [^{14}C]Asp in the C-terminal FLAG peptide, were detected by autoradiography. Due to the basic conditions (pH 8.5) of the tricine-SDS-PAGE running buffer, each observed band derived from E1–E9 was likely the corresponding $(ha)_n$-FLAG peptide(s) generated by the hydrolysis of full-length polyester. Note that the mobility of the peptide or polyester-peptide hybrid was dependent upon its composition, that is, the net charge or hydrophobicity, and therefore the peptide mobility did not accurately reflect the peptide length. The combination of ha-tRNAs used in each lane for polyester synthesis was as follows: lane 7, F^{lac}-$tRNA^{Asn\text{-}E1}_{GUU}$, mF^{lac}-$tRNA^{Asn\text{-}E1}_{GAC}$, and L^{lac}-$tRNA^{Asn\text{-}E2}_{GAA}$; lane 9, cF^{lac}-$tRNA^{Asn\text{-}E1}_{ACU}$, mF^{lac}-$tRNA^{Asn\text{-}E1}_{GAC}$, and A^{lac}-$tRNA^{MLAsn}_{CUG}$; lane 11, cF^{lac}-$tRNA^{Asn\text{-}E1}_{ACU}$, G^{lac}-$tRNA^{Asn\text{-}E2}_{GGU}$, and pF^{lac}-$tRNA^{Asn\text{-}E2}_{GAG}$.

chain, we propose the following possibility. According to various experiments examining the kinetics of a single elongation of an α-hydroxy acid, the ester bond transfer rate is estimated to be at least one order of magnitude slower than its peptide counterpart [20, 21]. Moreover, the dissociation constant of F^{lac}-$tRNA^{Phe}$ (K_d = 30 μM) with EF-Tu-GTP is about two orders of magnitude higher than that of Phe-$tRNA^{Phe}$ (K_d = 100 nM) [22]. Even though we attempted to compensate for the poor affinity of ha-tRNA for EF-Tu by increasing the concentration of ha-tRNA, these efforts were insufficient. Therefore, this combination of a slow esteryl transfer rate for α-hydroxy acids with the poor affinity of ha-tRNA for EF-Tu likely causes the ribosome to stall during the translation of long polyesters, possibly resulting in the frequent dissociation of the translation complex and polyesteryl-tRNA molecule from the mRNA template. Our observation that polyester yield correlated with polyester length appears to support this hypothesis. Detailed studies in the future should provide not only more insights into the mechanism but also insights into how to engineer the translation system toward a more efficient synthesis of longer polyesters.

One obvious strategy toward generating a more efficient translation system for polyester synthesis would be to engineer EF-Tu or orthogonal tRNAs to have a tighter binding affinity [23, 24]. Another possible strategy is to generate a mutant ribosome capable of catalyzing the esteryl transfer reaction more efficiently [25–27]. Thus, if we were able to optimize the affinity of ha-tRNA for EF-Tu and ribosomes by selection or increase the

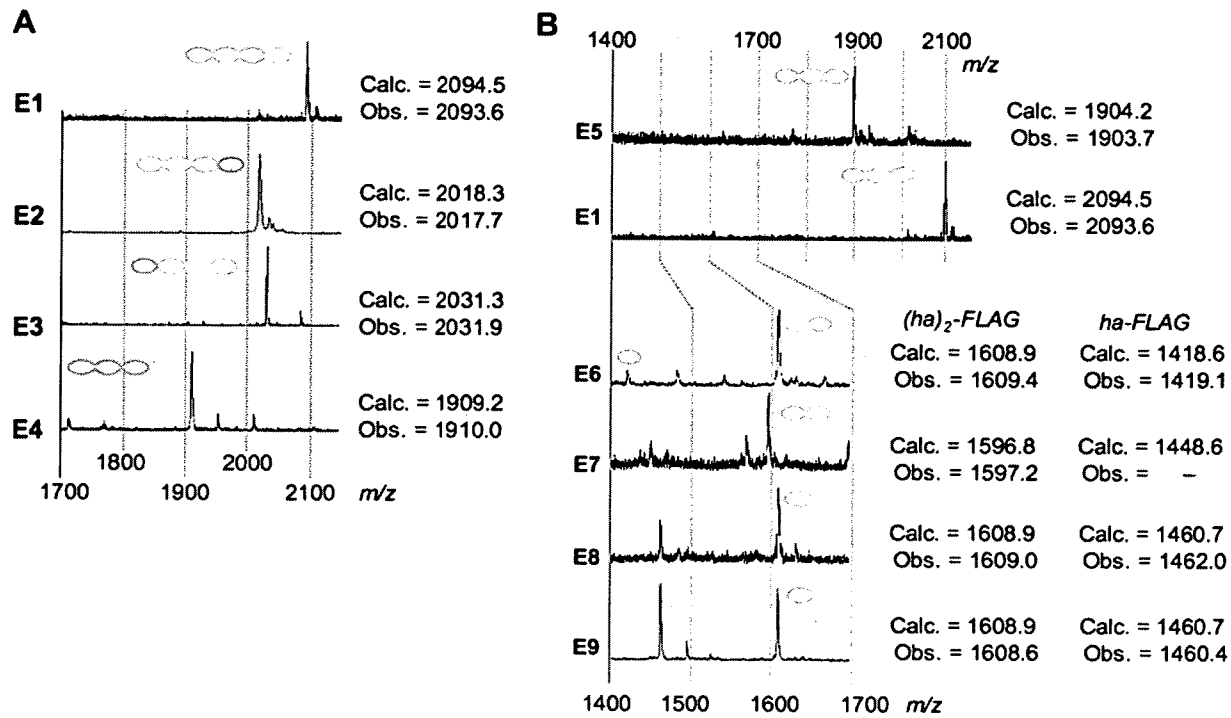

Figure 5. MALDI-TOF Analysis of Polyesters

(A) MALDI-TOF spectra of E1–E4. Calculated mass (M+H) and observed mass (M+H) are presented with the polyester moiety color-coded based on the reprogrammed genetic table shown in Figure 2A.

(B) MALDI-TOF spectra of E1 and E5–E9. Calculated mass (M+H) and observed mass (M+H) of full-length (E1 and E5) or $(ha)_2$-FLAG and ha-FLAG (E6–E9) are shown for each spectrum. The fragmented N-terminal products were removed during the FLAG-purification step, and therefore only the C-terminal fragments appear in the spectra.

efficiency of ribosomes for the esteryl transfer reaction, the translation system could be turned into a more efficient template-directed synthesizer for polyesters or even other nonpeptide biopolymers.

In light of the fact that polyesters have significantly different properties compared to peptides in terms of plasticity and rigidity, it is intriguing to investigate polyesters and polyester-polypeptide hybrid biopolymers engineered with a wide variety of side chains in strictly controlled sequences and lengths. However, because it has been difficult to synthesize such biopolymers with a variety of side chains, such biopolymers have not been well studied. The methodologies described in this report should open the door for the synthesis of a wide variety of polyesters and hybrid polymers, and thus will enable us to screen them for new possible functions and applications in the future.

SIGNIFICANCE

We have reported the mRNA-directed synthesis of polyesters, composed of several different α-hydroxy acids, whose sequence and length are fully controlled through reprogramming of the genetic code. This approach should be extendable to programmed synthesis of other types of backbone-modified biopolymers, such as polypeptide-ester hybrids and N-methyl-polypeptides.

EXPERIMENTAL PROCEDURES

α-Hydroxy Acid Substrate Synthesis

L-phenyllactic acid (F^{lac}) and lactic acid (A^{lac}) were purchased from Sigma-Aldrich and glycolic acid (G^{lac}) was purchase from Wako, Japan. *p*-isopropylphenyllactic acid (pF^{lac}), *p*-methoxyphenyllactic acid (mF^{lac}), and *p*-cyanophenyllactic (cF^{lac}) acid were synthesized from *p*-isopropylbenzaldehyde, *p*-methoxybenzaldehyde, and *p*-cyanobenzaldehyde, respectively, as previously reported [28]. *p*-isopropyllactic acid (L^{lac}) was synthesized as previously described [29]. All of the phenyllactic acid derivatives were converted to cyanomethyl ester (LG^1), and G^{lac}, A^{lac}, and L^{lac} were converted to dinitrobenzyl ester (LG^2) by the procedure reported elsewhere [14, 17].

Hydroxyacyl-tRNA Synthesis

For the hydroxyacylation of phenyllactic acid-LG^1 derivatives (F^{lac}, mF^{lac}, pF^{lac}, and cF^{lac}) eFlexiresin was used, whereas for other α-hydroxy acid-LG^2 derivatives (G^{lac}, L^{lac}, and A^{lac}) dFlexiresin was used. Due to the fact that tRNA hydroxyacylation was performed in the same manner regardless of either eFlexiresin or dFlexiresin, we refer to these resins commonly as Flexiresin in the protocol described below. Note that a general protocol for the preparation of Flexiresin is described in Supplemental Experimental Procedures. Hydroxyacylation was carried out as follows: a solution of 20 μl of 50 μM tRNA and 3 μl of 1 M Tris-HCl (pH 8.0) was heated at 95°C for 2 min and cooled to room temperature over 5 min. Six microliters of 3 M $MgCl_2$ was added to this mixture and the resulting solution was then loaded onto 10 μl (resin volume) of Flexiresin. After a suspension was made, the mixture was placed on ice and incubated for 5 min. The charging reaction was initiated by the addition of 1 μl of 300 mM α-hydroxy acid activated with an appropriate leaving group (LG^1 or LG^2) in

DMSO, and the mixture was incubated for 3 hr on ice. When *p*-isopropyllactic acid-LG[2] (L^{lac}) was used as a substrate, the reaction was incubated for 16 hr. Following the incubation, the supernatant was removed and Flexiresin-bound ha-tRNA was eluted with 30 μl of elution buffer (50 mM HEPES-K [pH 7.5], 10 mM EDTA) four times. To the pooled eluate 13.3 μl of 3 M NaOAc (pH 5.2) was added, and the resulting solution was precipitated with 280 μl of ethanol. After centrifugation, the resulting pellet was washed with 70% ethanol and dried under vacuum. Typically, the resulting ha-tRNA was dissolved in 0.5 μl of water to perform the expression of polyesters.

mRNA-Directed Polyester Synthesis

The *w*PURE system contains all the necessary components for translation except for AlaRS, ArgRS, AsnRS, CysRS, GlnRS, GluRS, GlyRS, HisRS, IleRS, LeuRS, PheRS, ProRS, SerRS, ThrRS, TrpRS, ValRS, and all 20 standard amino acids. To 12.6 μl of the above *w*PURE system was added 3.0 μl of 0.4 μM template DNA, 0.5 μl of 180 mM EDTA (pH 8.0), 3.0 μl of the mixture of Met, Tyr, and Lys (2 mM each), and 2.4 μl of 2 mM Asp (for MALDI-TOF analysis) or 500 μM [^{14}C]Asp (for tricine-SDS-PAGE assay). The mixture of ha-tRNAs (approximately 1000 pmol each) dissolved in 1.5 μl of 1 mM NaOAc (pH 5.2) was added to 3.5 μl of the above stock solution (total 5 μl translation volume) and the resulting mixture was incubated for 3 hr at 37°C. The synthesis of polyesters was then analyzed by the following procedures.

SDS-PAGE Analysis

The gel dimensions were as follows. The lengths of separation and stacking gels were approximately 55 and 10 mm, respectively, and the width and thickness were 83 and 0.75 mm, respectively. Separation gels contained 15% acrylamide (acrylamide:bisacrylamide = 19:1), 1 M Tris-HCl (pH 8.5), 0.1% SDS, and 13% glycerol, whereas the stacking gels contained 4% acrylamide (acrylamide:bisacrylamide = 29:1), 0.75 M Tris-HCl (pH 8.5), and 0.075% SDS. Electrophoresis was performed for 80 min under 20 mA constant mode. The anode running buffer was 200 mM Tris-HCl (pH 8.9), whereas the cathode running buffer contained 100 mM Tris, 100 mM tricine, and 0.1% SDS (the resulting buffer was approximately pH 8.3). The products labeled with [^{14}C]Asp in the C-terminal FLAG peptide were quantified by autoradiography using an image analyzer (FLA-5100, Fuji, Japan).

MALDI-TOF Analysis

The expressed product was incubated with FLAG-M2 agarose (Sigma) and the resin was washed with 50 μl of washing buffer (50 mM MOPS-K [pH 7.0], 150 mM NaCl). The immobilized product was eluted with 10 μl of 0.2% TFA. The purified product was then desalted with ZipTip$_{\mu\text{-}C18}$ (Millipore), and eluted with 1 μl of a 50% MeCN, 0.1% TFA solution saturated with the matrix *R*-cyano-4-hydroxycinnamic acid. MALDI-MS measurement of each product was performed using Autoflex II TOF/TOF (Bruker Daltonics) under the linear/positive mode and externally calibrated with Substance P (1347.5354 Da), Bombesin (1619.8223 Da), ACTH clip (1–17) (2093.0862 Da), and ACTH clip (18–39) (2465.1983 Da) as standards.

Supplemental Data

Supplemental Data include two figures and Supplemental Experimental Procedures and can be found with this article online at http://www.chembiol.com/cgi/content/full/14/12/1315/DC1/.

ACKNOWLEDGMENTS

We thank Professor M. Komiyama for the MALDI instrumentation and Dr. Patrick C. Reid for proofreading. This work was supported by grants from the Japan Society for the Promotion of Science Grants-in-Aid for Scientific Research (S) (16101007) and the U.S. National Institutes of Health (GM59159).

Received: May 30, 2007
Revised: September 11, 2007
Accepted: October 22, 2007
Published: December 26, 2007

REFERENCES

1. Josephson, K., Hartman, M.C., and Szostak, J.W. (2005). Ribosomal synthesis of unnatural peptides. J. Am. Chem. Soc. *127*, 11727–11735.
2. Forster, A.C., Tan, Z., Nalam, M.N., Lin, H., Qu, H., Cornish, V.W., and Blacklow, S.C. (2003). Programming peptidomimetic syntheses by translating genetic codes designed de novo. Proc. Natl. Acad. Sci. USA *100*, 6353–6357.
3. Frankel, A., Millward, S.W., and Roberts, R.W. (2003). Encodamers: unnatural peptide oligomers encoded in RNA. Chem. Biol. *10*, 1043–1050.
4. Merryman, C., and Green, R. (2004). Transformation of aminoacyl tRNAs for the in vitro selection of "drug-like" molecules. Chem. Biol. *11*, 575–582.
5. Kwon, I., Kirshenbaum, K., and Tirrell, D.A. (2003). Breaking the degeneracy of the genetic code. J. Am. Chem. Soc. *125*, 7512–7513.
6. Seebeck, F.P., and Szostak, J.W. (2006). Ribosomal synthesis of dehydroalanine-containing peptides. J. Am. Chem. Soc. *128*, 7150–7151.
7. Ellman, J.A., Mendel, D., and Schultz, P.G. (1992). Site-specific incorporation of novel backbone structures into proteins. Science *255*, 197–200.
8. Koh, J.T., Cornish, V.W., and Schultz, P.G. (1997). An experimental approach to evaluating the role of backbone interactions in proteins using unnatural amino acid mutagenesis. Biochemistry *36*, 11314–11322.
9. Tan, Z., Forster, A.C., Blacklow, S.C., and Cornish, V.W. (2004). Amino acid backbone specificity of the *Escherichia coli* translation machinery. J. Am. Chem. Soc. *126*, 12752–12753.
10. England, P.M., Lester, H.A., and Dougherty, D.A. (1999). Mapping disulfide connectivity using backbone ester hydrolysis. Biochemistry *38*, 14409–14415.
11. Fahnestock, S., and Rich, A. (1971). Synthesis by ribosomes of viral coat protein containing ester linkages. Nat. New Biol. *229*, 8–10.
12. Fahnestock, S., and Rich, A. (1971). Ribosome-catalyzed polyester formation. Science *173*, 340–343.
13. Millward, S.W., Takahashi, T.T., and Roberts, R.W. (2005). A general route for post-translational cyclization of mRNA display libraries. J. Am. Chem. Soc. *127*, 14142–14143.
14. Murakami, H., Ohta, A., Ashigai, H., and Suga, H. (2006). A highly flexible tRNA acylation method for non-natural polypeptide synthesis. Nat. Methods *3*, 357–359.
15. Murakami, H., Kourouklis, D., and Suga, H. (2003). Using a solid-phase ribozyme aminoacylation system to reprogram the genetic code. Chem. Biol. *10*, 1077–1084.
16. Murakami, H., Saito, H., and Suga, H. (2003). A versatile tRNA aminoacylation catalyst based on RNA. Chem. Biol. *10*, 655–662.
17. Saito, H., Kourouklis, D., and Suga, H. (2001). An in vitro evolved precursor tRNA with aminoacylation activity. EMBO J. *20*, 1797–1806.
18. Shimizu, Y., Inoue, A., Tomari, Y., Suzuki, T., Yokogawa, T., Nishikawa, K., and Ueda, T. (2001). Cell-free translation reconstituted with purified components. Nat. Biotechnol. *19*, 751–755.
19. Forster, A.C., Weissbach, H., and Blacklow, S.C. (2001). A simplified reconstitution of mRNA-directed peptide synthesis: activity of

the ε enhancer and an unnatural amino acid. Anal. Biochem. *297*, 60–70.

20. Fahnestock, S., Neumann, H., Shashoua, V., and Rich, A. (1970). Ribosome-catalyzed ester formation. Biochemistry *9*, 2477–2483.
21. Bieling, P., Beringer, M., Adio, S., and Rodnina, M.V. (2006). Peptide bond formation does not involve acid-base catalysis by ribosomal residues. Nat. Struct. Mol. Biol. *13*, 423–428.
22. Derwenskus, K.H., and Sprinzl, M. (1983). Interaction of cinnamyl-tRNAPhe with *Escherichia coli* elongation factor Tu. FEBS Lett. *151*, 143–147.
23. LaRiviere, F.J., Wolfson, A.D., and Uhlenbeck, O.C. (2001). Uniform binding of aminoacyl-tRNAs to elongation factor Tu by thermodynamic compensation. Science *294*, 165–168.
24. Asahara, H., and Uhlenbeck, O.C. (2002). The tRNA specificity of *Thermus thermophilus* EF-Tu. Proc. Natl. Acad. Sci. USA *99*, 3499–3504.
25. Cochella, L., and Green, R. (2004). Isolation of antibiotic resistance mutations in the rRNA by using an in vitro selection system. Proc. Natl. Acad. Sci. USA *101*, 3786–3791.
26. Dedkova, L.M., Fahmi, N.E., Golovine, S.Y., and Hecht, S.M. (2003). Enhanced D-amino acid incorporation into protein by modified ribosomes. J. Am. Chem. Soc. *125*, 6616–6617.
27. Dedkova, L.M., Fahmi, N.E., Golovine, S.Y., and Hecht, S.M. (2006). Construction of modified ribosomes for incorporation of D-amino acids into proteins. Biochemistry *45*, 15541–15551.
28. Dahn, H., and Rotzler, G. (1991). Unstable 1,1,2-enetriols as (probable) intermediates in the decarboxylation of α,β-diketo acids. J. Org. Chem. *56*, 3080–3082.
29. Deechongkit, S., You, S.L., and Kelly, J.W. (2004). Synthesis of all nineteen appropriately protected chiral α-hydroxy acid equivalents of the α-amino acids for Boc solid-phase depsi-peptide synthesis. Org. Lett. *6*, 497–500.

Cell PRESS

Chemistry & Biology
Article

Messenger RNA-Programmed Incorporation of Multiple N-Methyl-Amino Acids into Linear and Cyclic Peptides

Takashi Kawakami,[1] Hiroshi Murakami,[2] and Hiroaki Suga[1,2,*]
[1]Department of Chemistry and Biotechnology, Graduate School of Engineering, The University of Tokyo, Tokyo 113-8656, Japan
[2]Research Center for Advanced Science and Technology, The University of Tokyo, Tokyo 153-0894, Japan
*Correspondence: hsuga@rcast.u-tokyo.ac.jp
DOI 10.1016/j.chembiol.2007.12.008

SUMMARY

Natural peptide products often contain N-methylated backbones, and such a modification plays a crucial role in making natural peptides peptidase resistant and membrane permeable. Here, we demonstrate the ribosomal synthesis of N-methyl-peptides by means of genetic code reprogramming. Two key technologies, a ribozyme-based de novo tRNA acylation (flexizyme) system and an *E. coli* reconstituted cell-free translation (PURE) system, were used in order to reassign arbitrarily chosen codons to N^{α}-methylated amino acids (^{Me}aa). Using this combination, we determined the general structural requirement of "accessible" ^{Me}aa and demonstrated their multiple incorporations into the nascent peptide chain according to the assignments made on mRNA, giving linear and cyclic N-methyl-peptides in high purities. This platform technology offers a convenient tool for the construction of N-methyl-peptide libraries, potentially leading to the discovery of therapeutic peptides.

INTRODUCTION

Natural peptide products isolated from various organisms often contain N-methylated backbones (Billich and Zocher, 1990; Hornbogen and Zocher, 2005). Such a modification of peptide backbone alters the properties of the peptide bond, which confers their conformational rigidity (Sagan et al., 2004). This modification contributes to improvements in the biological properties of natural peptides, such as target affinity, proteolytic stability, and/or membrane permeability. Thus, N^{α}-methylated amino acids (^{Me}aa) are invaluable components for the synthesis of peptide libraries in screening for peptides with suitable drug-like properties for potential therapeutic use. The backbone N-methylation of these peptides are generally executed by one or more of enzymes in the multienzyme clusters, called nonribosomal peptide synthetases (NRPSs) (Billich and Zocher, 1990; Hornbogen and Zocher, 2005; Sieber and Marahiel, 2005; Walsh et al., 2001). This type of peptide synthesis machinery is known to be template independent, in contrast to the mRNA template-dependent ribosomal machinery. Unfortunately, their complexity demands an enormous effort to manipulate the systems, thereby making it difficult to generate desired peptide libraries (Baltz, 2006; Fischbach and Walsh, 2006; Hahn and Stachelhaus, 2006).

On the other hand, the translation machinery expresses peptides in an mRNA template-dependent manner, which makes this system exceptionally versatile and useful for the synthesis of peptides or proteins. Unlike NRPSs, the ordinary translation system strictly incorporates 20 proteinogenic amino acids into the nascent peptide chain. However, an appropriate manipulation of the translation apparatus enables us to incorporate nonproteinogenic amino acids into peptides (Hendrickson et al., 2004; Hohsaka and Sisido, 2002; Link et al., 2003; Wang and Schultz, 2004). A classical example is that when a nonproteinogenic amino acid is charged onto an orthogonal $tRNA_{CUA}$ (the subscript base sequence indicates the anticodon), this aminoacyl-$tRNA_{CUA}$ (aa-$tRNA_{CUA}$) is able to suppress UAG amber stop codon on mRNA; thereby, the amino acid can be incorporated into the nascent peptide at the designated site (Bain et al., 1989; Noren et al., 1989). Despite encouraging results from a number of successful examples for the incorporation of nonproteinogenic amino acids with various nonnatural side chains, it has been known that some ^{Me}aa are incorporated into a peptide chain with good or modest efficiencies, and some are not at all (Bain et al., 1991; Chung et al., 1993; Ellman et al., 1992; Gilmore et al., 1999; Karginov et al., 1997; Mendel et al., 1995; Murakami et al., 2006; Short et al., 2000). To the best of our knowledge in the literature, only three ^{Me}aa, ^{Me}Gly, ^{Me}Ala, and ^{Me}Phe, have been successfully incorporated into the nascent peptide chain by means of amber suppression. Moreover, neither incorporation of multiple ^{Me}aa nor a single ^{Me}aa with amino acids bearing noncanonical side chains has been thus far reported.

More recently, a new concept of genetic code reprogramming was introduced by Forster et al. and applied to the incorporation of nonproteinogenic amino acids into peptides (Forster et al., 2003). Genetic code reprogramming involves the reassignment of codons from proteinogenic amino acids to nonproteinogenic ones via multiple sense suppressions. Thus, this methodology enables us to simultaneously incorporate multiple nonproteinogenic amino acids into peptides, which represents a major advantage over the aforementioned amber suppression method (Forster et al., 2003; Josephson et al., 2005; Murakami et al., 2006; Ohta et al., 2007; Ohuchi et al., 2007; Tan et al., 2005).

In the context of ^{Me}aa using the sense suppressions, there were three examples in the literature (Frankel et al., 2003; Merryman and Green, 2004; Tan et al., 2004). Merryman and Green have reported that aa-tRNAs prepared by cognate aminoactyl-tRNA

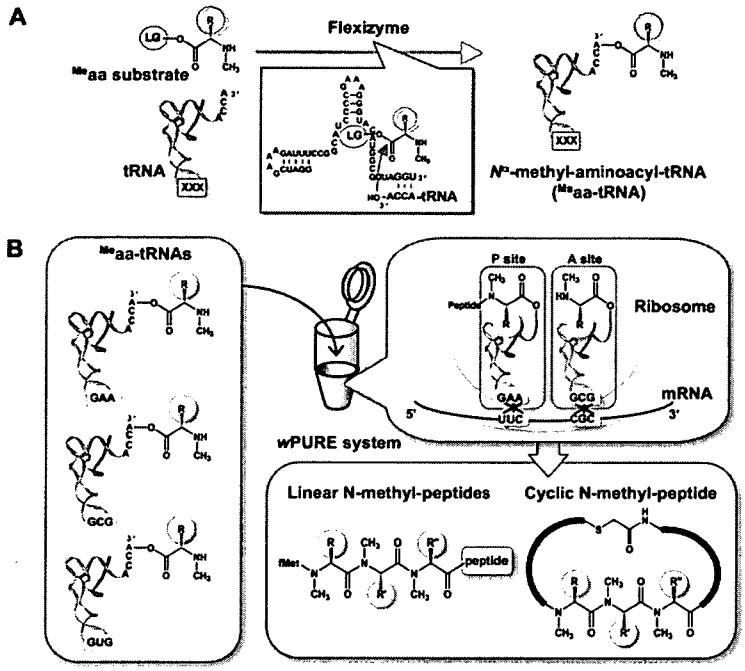

Figure 1. Messenger RNA-Programmed Synthesis of N-Methyl-Peptides by Genetic Code Reprogramming

(A) Synthesis of N^{α}-methyl-aminoacyl-tRNA (^{Me}aa-tRNA) by flexizyme system. Flexizyme recognizes leaving group (LG: highlighted in pink) on the ester bond of N^{α}-methyl-amino acid (^{Me}aa) substrate and conserved three bases on the 3′-terminus of tRNA, which allows for the aminoacylation of desired tRNA with any ^{Me}aa. N^{α}-methyl groups are highlighted in yellow.

(B) Ribosomal synthesis of N-methyl-peptide. ^{Me}aa-tRNAs bearing various combinations of ^{Me}aa and anticodon are added to the *w*PURE (*withdrawn* protein synthesis using recombinant elements) system for mRNA-programmed incorporation of ^{Me}aa into peptides. The *w*PURE system is an *E. coli* reconstituted cell-free translation system in which some components (amino acids and aminoacyl-tRNA synthases) are withdrawn from the ordinary translation system to reassign multiple sense codons to various ^{Me}aa.

(C) Reprogrammed genetic code table for the mRNA-programmed synthesis of N-methyl-peptides. Codons that are reassigned to various ^{Me}aa are shown in color letters. Initiation codon (AUG) highlighted in gray is reassigned from Met to N^{α}-(α-chloroacetyl)-Phe (^{ClAc}Phe) for the ribosomal synthesis of cyclic N-methyl-peptides.

synthetases (aaRSs) were converted to ^{Me}aa-tRNAs by the three-step procedure, where the α-amino group was alkylated by consecutive reductive amination with 2-nitrobenzaldehyde and formaldehyde, and then the 2-nitrobenzyl group was deprotected by UV irradiation (Merryman and Green, 2004). These ^{Me}aa-tRNAs derived from 20 proteinogenic amino acids were surveyed for the synthesis of a dipeptide, fMet-^{Me}aa, where thin-layer chromatographic electrophoresis was mainly used to discern the product of fMet-^{Me}aa from fMet (also possibly fMet-aa) and to determine the incorporation efficiency of each ^{Me}aa in a semiquantitative manner. In the second example, Tan and Cornish et al. prepared ^{Me}Ala-tRNA$^{AsnB}_{GAC}$ and ^{Me}Phe-tRNA$^{AsnB}_{GAC}$ by the chemoenzymatic aminoacylation procedure (Hecht et al., 1978; Robertson et al., 1991) and performed their single incorporation into a tripeptide (fMet-Xaa-Glu, where Xaa represents ^{Me}aa) upon the sense suppression of the Val codon (GUU) (Tan et al., 2004). Significantly, this work determined the incorporation efficiencies of these two ^{Me}aa into the peptide chain in a quantitative manner and also confirmed the product peptide by liquid chromatography based on its retention time by comparison with that of the corresponding synthetic authentic sample. Both examples above showed only a single incorporation of ^{Me}aa into a di- or tripeptide backbone, and therefore the concept of genetic code reprogramming has not yet been fully explored for the synthesis of N-methyl-peptides.

In the third example, Frankel and Roberts et al. have shown polymerization of ^{Me}Phe assigned to in repetition of two, five, or ten residues in an in vitro display system (Frankel et al., 2003). This work represents, to our knowledge, the first demonstration of consecutive incorporations of a single type of ^{Me}aa into a peptide stretch by using sense suppression. However, because the polymerization of ^{Me}Phe was only evidenced by observing the protease resistance of the respective peptide, it still remains unknown to what degree of the contamination of natural amino acids in the poly-^{Me}Phe chain occurred. In fact, the full-length peptide bearing multiple ^{Me}Phe was susceptible to protease to some extent, suggesting that competing incorporations of likely Val or possibly other proteinogenic amino acids occurred as Frankel et al. discussed in their report (Frankel et al., 2003). Taken together, although the above three examples clearly documented that the sense-suppression method could be used for the incorporation of ^{Me}aa, the proof-of-concept study on the genetic code reprogramming, i.e., performing multiple incorporations of two or more different ^{Me}aa with high fidelity control, remains to be demonstrated.

We report here incorporation of multiple ^{Me}aa into the peptide backbone with a nearly perfect control of sequences and lengths by using the concept of genetic code reprogramming. To reprogram the genetic code, we used two technologies, flexizyme and PURE (protein synthesis using recombinant elements) systems. Flexizyme system is a ribozyme-based de novo tRNA acylation system that is able to charge virtually any amino acids onto desired tRNAs with any body and anticodon sequences (Figure 1A) (Kourouklis et al., 2005; Murakami et al., 2003a, 2003b, 2006; Ohuchi et al., 2007; Saito et al., 2001). PURE system is a